Effects of density of doping level on the electrical properties of the near-surface region of p-type Gallium Antimonide (GaSb)

By

Dereje Assefa Kebede

Adama, Ethiopia

October 2019

Effects of density of doping level on the Electrical Properties of the near-surface region P-type Gallium Antimonide (GaSb)

By

Dereje Assefa Kebede

Advisor

Dr. Megersa Wodajo Shura

A Thesis Submitted to Applied Physics Program

Partial School of Applied Natural Science

Presented in Partial Fulfilment of The Requirements For The Degree of Masters of Science in Physics

Office of Graduates' Studies

Adama Science and Technology University

Adama, Ethiopia

October 2019

ADAMA SCIENCE AND TECHNOLOGY UNIVERSITY

POSTGRADUATE PROGRAM

SCHOOL OF APPLIED NATURAL SCIENCE

APPLIED PHYSICS PROGRAM

As a thesis research advisor, I hereby certify that I have read and evaluated this thesis entitled: "**Effects of density of doping level on the electrical properties of the near-surface region of p-type Gallium Antimonide (GaSb)**" prepared under my guidance by Dereje Assefa. I recommend that it can be submitted as fulfilling the thesis requirement.

Dr. Megersa Wodajo _____ _____

Advisor Signature Date

As members of the Board of Examiners of the M.Sc. thesis Open Defense Examination, we certify that we have read and evaluated the thesis work prepared by Dereje Assefa and examined the candidate. We recommended that the thesis is accepted as fulfilling the thesis requirement for the Degree of Master of Science in Physics.

_____ _____ _____

Chairperson Signature Date

_____ _____ _____

Internal Examiner Signature Date

_____ _____ _____

External Examiner Signature Date

Declaration and statement of the candidate

I hereby declare that this draft is entirely my own and does not contain material from unreferenced external sources (including the work of other students or professional interventions) and this draft has never been submitted elsewhere for academic credit.

All sources employed in this draft including the internet and all paraphrased text sources have been correctly referenced in the citation and bibliography. This thesis is a presentation of my original research work. Wherever contributions of others are involved, every effort is made to indicate this clearly, with due reference to the literature, and acknowledgment of collaborative research and discussions. Brief lines from this thesis are permissible without distinct permission provided that accurate acknowledgment of source is made. In all other occasions, however, permission must be obtained from the author.

Candidate`s name: Dereje Assefa Kebede Signature_____

Place: Adama science and Technology University, Adama

Date of Submission: October, 2019

Acknowledgments

First and foremost, I would like to thank Almighty God for giving me the strength, knowledge, ability and opportunity to undertake persevere and complete it successfully. Next, my deepest gratitude goes to my former teacher and advisor Assistant professor, Dr. Megersa Wodajo for his so great support, guidance, and constructive criticisms together with irreplaceable supervision and inspiration, without whom this thesis would not have been possible. I honestly express my humble gratitude to all my instructors at ASTU, examiners for their willingness to spare their time and skill so as to guide me to complete my study. I extend my sincere gratitude to Adama Science and Technology University (ASTU) applied physics postgraduate, PG library workers and officers who peacefully show me endurance during my stay in the University.

My acknowledgment would be incomplete without thanking the biggest source of my strength, my darling wife Hirut Bekele who always suits me by maintaining me strong through her prayer, financial support and carrying all the burdens of life lonely when I am off from home for study. I would never have had the strength to accomplish this major life goal without her devotion and sacrifices whilst taking on all my responsibilities.

I also would like to convey my appreciation to my lovely kids, Aviela Dereje, Eliora Dereje and Lewi Dereje for their endless love and overcoming solitude when I am off. Finally, I am also hugely appreciative to everyone who has been a part of my life directly or indirectly supported and prayed for me along the way.

Table of Contents

Contents Page

List of Figures

Figures Page

List of Symbols and Abbreviations

E_g	Energy bandgap
E_C	Energy of Conduction band edge
E_V	Energy of Valence band edge
T	Temperature
k_B	Boltzmann's constant
m_n	Mass of electron
m_n*	Effective mass of electron
m_p *	Effective mass of hole
E_{g0}	Bandgap energy at zero kelvin
$E_g(T)$	Bandgap energy at any temperature
α	Temperature coefficient of semiconductors
β	Fitting parameter of the energy band gap
N_C	Effective density of holes in conduction band
N_V	Effective density of electron in the valence band
ρ_C	Total density of states in conduction band
ρ_V	Total density of states in valence band
p_0	Total density of holes in valence band
n_0	Total density of electrons in conduction band
n	Number of excited electrons in conduction band
p	Number of excited holes in valence band
n_i	Intrinsic carrier concentration
h	Planck's constant
N_a	Density of electrons occupying acceptor states
p_a	Density of holes bound to acceptors
N_a^-	Concentration of ionized acceptors
n_d	Density of electrons occupying donor states
N_d^+	Concentration of ionized donors
n_R	Concentration of total EHP annihilated after ionization

$\Re$	Concentration of EHP thermally generated from band to band
E_i	Intrinsic energy
E_F	Fermi level energy
E_{SF}	The surface Fermi level energy
k	The wave vector
T_D	The Debye temperature
E_a	Energy of acceptor level relative to the valence band
E_d	Energy of donor level relative to the conduction band
g_a	The degeneracy factor of acceptor ions
g_d	The degeneracy factor of donor ions
k_∞	Dielectric constant at high frequency
a_0	Lattice constant
b_1	Total depletion width
b_δ	The width of the transition layer
b_S	The width of the highly depleted layer
e	The electron charge
$\bar{N}_1$	The charge density near the quasi-neutral region
$\bar{N}_\delta$	The charge density in the transition layer
$\bar{N}_S$	The charge density near the surface region
E_δ	The energy bending in the transition layer
E_S	The energy bending near the quasi-neutral region
E_{kn}	Kinetic energy of free electrons
E_{kp}	Kinetic energy of free holes
E	Total energy of free carriers
E_0	Reference energy of free carries
$V(x)$	Electrostatic potential at any point
V_0	Electrostatic potential at x = 0
$\varepsilon(x)$	Electric field intensity function at any point in the depletion region
ε_S	Electric field intensity as a function of position near surface
ε_1	Electric field intensity as a function of position near quasi-neutral region

ε_δ	Electric field intensity as a function of position in the transition layer
$\bar{N}(x)$	Average volume charge density
$p_0(x)$	Majority carrier density as a function of position
$E_V(x)$	Valence band energy at any point in the depletion region
ΔE	Change energy in any two positions
E_{V0}	Valence band energy at thermal equilibrium
$E(x)$	Energy function at any point in the depletion region
x	Depth below the surface
R	Total recombination of electron-hole-pairs
R_{eeh}	Auger recombination due to two electrons and a hole
R_{ehh}	Auger recombination due to two holes and an electron
C_R	Radiative recombination capture coefficient
σ	Surface charge density
R_0	Thermal equilibrium recombination rate
U	Total recombination rate
U_A	Auger recombination rate
δn	Photogenerated excess carrier electrons
δp	Photogenerated excess carrier holes
τ_R	Radiative recombination excess carrier lifetime
τ_A	Auger recombination excess carrier lifetime
τ_{R0}	Photogenerated radiative excess carrier lifetime
τ_{A0}	Photogenerated auger excess carrier lifetime
τ_k	Radiative recombination excess carrier time constant
k_A	Auger recombination excess carrier time constant
τ_{eff}	Effective excess carrier lifetime

Abstract

In this study, the variation of thermal equilibrium charge carrier densities and the net ionization density in the near-surface depletion with energy bending is described for p-type GaSb. The result indicates band bending increases with doping level. Applying gauss's law to both the surface and the near-surface region, the net electric field is not linearly varying with position, rather it is a deviated line. Using the relation between the one-dimensional potential gradient and the electric field, The electric field in the near-surface, the transition layer and near the quasi-neutral region are linearly varying with position. Using the fact that the electric field and the energy are zero at the boundary between the depletion layer and the quasi-neutral region, since the surface and volume charge density balance each other the values of the electric field, the energy, and the charge density at the surface are described in terms of the net ionization density inside the entire depletion layer. The value of the energy at the surface can be obtained as a function of doping level using the well-known relation between the bulk and the surface Fermi-level positions. Description of energy at the surface enables us to determine the values the net ionization densities near the surface, at the border between the highly depleted layer and the transition layer; and inside the entire depletion layer and the width of the depletion layer as function of doping density. Upon describing the energy as a function of position in the entire depletion layer, one can describe position dependences of the net ionization density, the carrier densities, the electric field strength and the excess carrier lifetimes in the entire depletion layer. The obtained result revealed that, the energy is bending down quadratically with position from the quasi-neutral region to the surface, the majority carrier density decreases exponentially with position from the quasi-neutral region to the surface, the electric field strength decreases non-linearly with position from the surface to the quasi-neutral region and the excess carrier lifetime decreases exponentially from the surface to the quasi-neutral region. The doping level affects the magnitudes of the surface charge density, the energy and the electric field in the entire depletion layer and the magnitudes of the carrier densities and the excess carrier lifetimes under the surface are found to be unaffected by the doping level of the material since the surface fermi pinning energy is taken a constant value.

Chapter 1 : Introduction

1.1 Background

Semiconducting materials have been of scientific attention for almost two centuries. The finding of semiconductors is generally skilled to Michael Faraday, who in 1833 published a report on a material with a resistivity which had the opposite temperature dependence to that typically measured for metals [1]. The semiconductor device has a fairly long history, although the greatest explosion of IC technology has occurred during the last two or three decades. The metal-semiconductor contact dates back to the early work of Braun in 1874, who discovered the asymmetric nature of electrical conduction between metal contacts and semiconductors, such as copper, iron, and lead sulfide. These devices were used as detectors. In 1906, Pickard took out a patent for a point contact detector using silicon and, one year ago in 1907, Pierce published rectification characteristics of diodes made by sputtering metals onto a variety of semiconductors [2]. By 1935, selenium rectifiers and silicon point-contact diodes were available for use as radio detectors. A significant advance in our understanding of the metal-semiconductor contact was aided by developments in semiconductor physics [3]. In 1942, Bethe developed the thermionic-emission theory, according to which the current is determined by the process of emission of electrons into the metal rather than by drift or diffusion [4].

Another big breakthrough came in December 1947 when the first transistor was constructed and tested at Bell Telephone Laboratories by William Shockley, John Bardeen, and Walter Brattain. This first transistor was a point contact device and used polycrystalline germanium. The transistor effect was soon demonstrated in silicon as well. A significant improvement occurred at the end of 1949 when single-crystal material was used rather than the polycrystalline material. The single crystal yields uniform and improved properties throughout the whole semiconductor materials [5].

The next significant step in the development of the transistor was the use of the diffusion process to form the necessary junctions. This process allowed better control of the transistor characteristics and yielded higher-frequency devices. The diffused metal transistor was

commercially available in germanium in 1957 and in silicon in 1958 [6]. The diffusion process also allowed many transistors to be fabricated on a single silicon slice, so the cost of these devices decreased [7].

The column IV elemental semiconductors, silicon and germanium are called elemental semiconductors because they are composed of single species of atoms. Compounds of column III and V atoms, as well as certain combinations from II and VI, and from IV and VI, and III and IV make up the compound semiconductors. Every solid has its own characteristic energy band structure. This variation in band structure is responsible for the wide range of electrical characteristics observed in various materials. In metals, the bands either overlap or are only partially filled. Thus, in metals, high electrical conductivity is due to the fact that electrons and empty energy states are intermixed within bands so that electrons can move freely under the influence of an electric field. Consider a valence band in the ground state. The total crystal momentum for this band is zero, as for every occupied k state; there exists a corresponding filled state with opposite momentum. The top of the valence band and bottom of the conduction band for most direct semiconductors occurs at zero k [8].

Binary compounds are mostly between elements in groups III and V (such as gallium antimonide), groups II and VI, (such as zinc sulfide), groups IV and VI, (such as zinc oxide). Certain ternary and quaternary compounds, oxides, and alloys also exist. Most common semiconducting materials are crystalline solids, but amorphous and liquid semiconductors are also known. These include hydrogenated amorphous silicon and mixtures of arsenic, selenium, and tellurium in a variety of proportions. These compounds share with better-known semiconductors the properties of intermediate conductivity and a rapid variation of conductivity with temperature, as well as occasional negative resistance [9].

Semiconductors are a group of materials having electrical conductivities intermediate between metals and insulators. It is significant that the conductivity of these materials can be varied over orders of magnitude by changes in temperature, optical excitation, and impurity content. This variability of electrical properties makes them natural choices for electronic device investigations [10].

The electrical conductivity of a semiconductor material increases with increasing temperature, which is behavior opposite to that of a metal. Semiconductor devices can

display a range of useful properties such as passing current more easily in one direction than the other, showing variable resistance, and sensitivity to light or heat. Because the electrical properties of a semiconductor material can be modified by controlled addition of impurities or by the application of electrical fields or light, devices made from semiconductors can be used for amplification, switching, and energy conversion. Current conduction in a semiconductor occurs through the movement of free electrons and "holes", collectively known as charge carriers [11].

For most of the device applications, semiconductor is doped with impurities. In the case of silicon, IV-group element, III or V-group elements are used as impurities. These impurities control the type and conductivity properties of silicon. Group III impurities act like acceptors and the group V impurities act like donors in silicon. The ionization energies of these impurities are low, and hence the energy level of these impurities are close to the band edge. Therefore, these impurities are generally referred to as shallow level impurities [12].
The Fermi level is an important consequence of band theory, the highest occupied quantum state of electrons at absolute zero temperature. The position of the Fermi level relative to the conduction band is an important parameter that contributes to determine the electrical properties of a particular material [13].

For a semiconductor, the electrical resistivity lies between a conductor and an insulator, i.e., in the range of 10^3 Siemens/cm to 10^8 Siemens/cm. An externally applied electrical field may change the semiconductor's resistivity. In conductors, current is carried by electrons, whereas in semiconductors, current is carried by the flow of electrons or positively charged holes [14].

The III–V compound semiconductors such as GaN, GaP, and GaAs are commonly used in light-emitting diodes (LEDs) whereas II-VI compound semiconductors such as ZnS are used in television screens as fluorescent materials. III-V semiconductors are used already in a number of appliances, most notably in optoelectronics and high electron mobility transistors (HEMT) in mobile communications. In optoelectronics, III-V's have many advantages compared to silicon. Most III-V semiconductors have a direct bandgap which is useful in light-emitting diodes and photovoltaic cells [15, 16, 17].

Many III-V semiconductors have higher electron mobility than silicon, which means higher drift velocity for electrons in III-V's as a function of the electric field applied. III-V compound semiconductors provide a wide range of band gaps. They vary from small bandgap materials e.g. InSb (0.17 eV) used in infrared detectors to large e.g. GaN (3.44 eV) and AlN (6.2) eV used in blue and ultraviolet LEDs and lasers. The bandgap can be either direct or indirect. The bandgap is direct if the valence band maximum (VBM) and conduction band minimum (CBM) locate at the same electron wave vector (k) [18].

Small direct band semiconductors with energy bandgap ranged from 0.18ev to 1.0ev, like indium arsenide (InAs), gallium antimonide (GaSb), and indium antimonide (InSb) are characterized by the absence or small amount of impurity materials, presence of very high charge carrier concentration. These materials are used in numerous domains, such as pollutant detection and infrared thermal imaging, using a variety of device architectures, including near-infrared photo-detectors, resonant tunneling structures, and other quantum devices [19].

Gallium antimonide (GaSb) and related compounds are suitable for fabricating high-frequency electronic and optoelectronic devices. The photoresponse of this material makes it very useful in the design of a variety of device architectures, including photodetectors, resonant tunneling structures, and other quantum devices. Some of these semiconductors are also used as booster cells in solar cell clusters to improve the efficiency of photovoltaic and thermo-photovoltaic cells. A great deal of civilization's hopes rest on continued technological advancement using semiconductors [20, 21].

Doping is the process of adding impurities to intrinsic semiconductors to alter their properties. Doping of a semiconducting material changes the electrical properties of a material. Using the relation between the one-dimensional potential gradient and the electric field, the variation of the energy in the depletion layer is described as functions of the surface charge density and the net ionization density near the surface. The doping level affects the magnitudes of the surface charge density, the energy and the electric field in the entire depletion layer whereas, the magnitudes of the carrier densities and the excess carrier lifetimes under the surface are found to be unaffected by the doping level of the material since the surface fermi pinning energy is taken a constant value [22].

1.2 Statement of the problem

The doping level dependence of the electric field in the entire depletion region as a function of position is used to determine the shape of electric field versus position in the near-surface depletion region. The electric field strength in the near-surface, in transition layer and the near quasi-neutral region as a function of position is linearly varying with position[23]. This research is aimed at determining the net electric field in the entire depletion region whether it is linearly or nonlinearly varying with position. No researches conducted displayed if it is non-linear.

1.3 Objectives of the Study

The general objective of this work is to determine the effects of the doping levels on the electrical properties of the near-surface depletion region in Gallium antimonide semiconductor.

The specific objectives are to describe the effect of doping level on:

- the energy,
- the charge carrier density,
- the electric field strength,
- the low injection level excess carrier lifetime in the entire depletion region.

1.4 Thesis Outline

The thesis is organized as follows: Chapter one offers the introduction part, chapter two presents the theoretical aspects of the thermal equilibrium properties and the semiconductors that are used in the analysis of this work. Chapter three describes the methods and procedures used to analyze the results of this work. Chapter four presents the discussion and analysis of the results. Chapter five provides the conclusion of the results obtained in chapter four.

Chapter 2 : Literature Reviews

2.1 Band Structure of GaSb

The band structure, effective masses, valence crystal binding, and transport properties are the most important features which describe the general nature of the GaSb compound semiconductor. The increased interest in this material may be explained by the unique feature of GaSb which include very narrow energy gaps, high mobility, and small effective masses of carriers and due to this the possibilities of practical applications in high-frequency semiconductor devices [24]. There is also considerable scientific interest in all mixed III-V compounds of Gallium series. The continuous variability of parameters in such kinds of materials makes possible the design of a material with virtually any gap width within the given range.

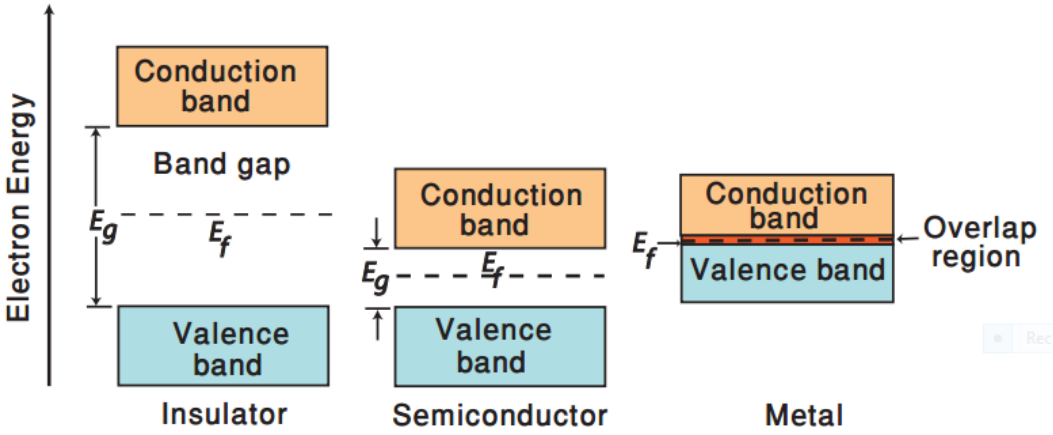

Figure 2.1: Simplified diagram of the electronic band structure of insulators, semiconductors, and metals. The position of the Fermi level is when the sample is at absolute zero temperature (0K) [25].

The design ability of such materials is especially useful for infrared or optical devices in which operation over particular wavelength ranges is required, such as in infrared sensors and injection lasers [26].

Gallium antimonide (GaSb) semiconductor material has received increasing attention because its wavelength covers a wide range of applications which go from 1.24 μm to 4.3 μm. It has turned out to be a promising material for the application in long-wavelength lasers and

photo-detectors for fiber optical communication system [27]. Consequently, it is an important candidate in high-speed applications in transistors and other devices [28, 29].

A zinc-blende structure is characteristically similar to a diamond lattice structure; however, alternating atoms are composed of different elements. The density of GaSb crystal is 5.61 $\frac{g}{cm^3}$ and the lattice constant a_0=6.096$\dot{A}$ [30].

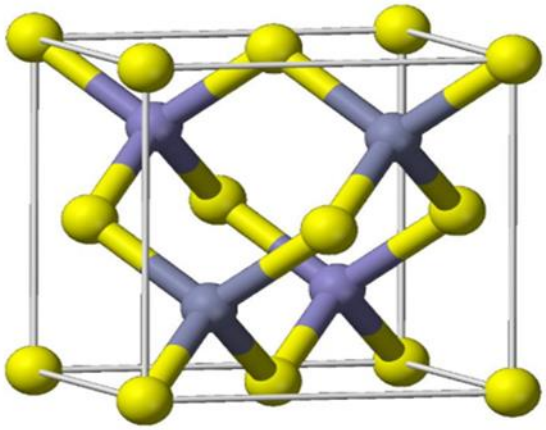

Figure 2.2: band structure of GaSb [31].

2.2 Energy bandgap

The available energies for electrons help us to differentiate between insulators, conductors and semiconductors. In free atoms, discrete energy levels are present, but in solid materials (such as insulators, semiconductors, and conductors) the available energy states are so close to one another that they form bands. The bandgap is an energy range where no electronic states are present. In insulators, the valence band is separated from the conduction band by a large gap, in good conductors such as metals the valence band overlaps the conduction band, whereas in semiconductors there is a small gap between the valence and conduction bands, small enough allowing thermal excitation of electrons from the valence to conduction band [32].

The position of the Fermi level is when the sample is at absolute zero temperature (0K). It depicts the top edge of the valence band, denoted by E_V, and the bottom edge of the conduction band, denoted by E_C . The difference between E_C and E_V is the bandgap energy or energy gap, E_g [33].

$$E_g = E_C - E_V, \tag{2-1}$$

Bandgap reductions with higher temperature mainly arise from the change of the lattice constant. So, as the lattice constant decreases, the interatomic distance will be reduced. The minimum energy that must be given to valence electrons to become a conduction electron is the energy gap [35].

The effect of temperature on band gap energy shrinkage has been quantified through several empirical or semiempirical relations. Among the empirical relationships, the Varshni relationship is often used to assess nonlinear temperature-dependent bandgap shift.. The Varshni equation for the bandgap variation as a function of temperature is: [36]

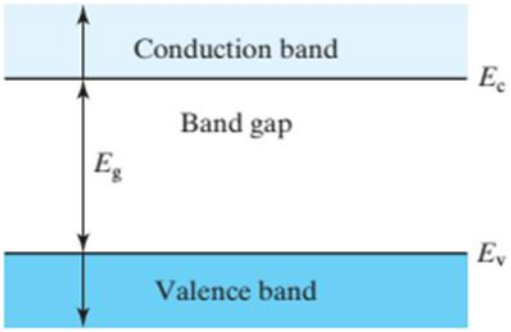

Figure 2.3: Simple schematic Energy diagram of conduction and valence bands [34].

$$E_g(T) = E_g(0) - \left(\frac{\alpha T^2}{\beta + T}\right) \qquad (2\text{-}2)$$

Where α and β are fitting parameters, with values $\alpha = 3.78\text{X}10^{-4}$eV/K and $\beta = 94$K which are characteristic of a given semiconductor. $E_g(0)$ is the bandgap of the semiconductor at zero kelvin (0K) which is 0.813eV for GaSb is the limiting value at zero Kelvin. The energy bandgap at room temperature (300K) for the same is known to be 0.726eV [37, 38].
Although this relation fits appropriately for various III-V and II-VI semiconductors, it gives negative values for the fitting parameters (A and B) for various known wide bandgap semiconductors. [39, 40].

Figure 2.3 shows the experimental bandgap shift as well as fitting using Eqn. (2-2), based on the Varshni model. It can be seen that the Varshni relation fits well for low temperatures (up to 360K); however, it shows deviation from experimental values, above 360K.

Furthermore, it illustrates the temperature dependence of bandgap energy along with E_C *and* E_V. As one can be seen from the figure, both E_C *and* E_V become closer and closer to the mid-gap with increasing temperature, this results in the increasing of the bandgap energy while the temperature keeps decreasing [42].

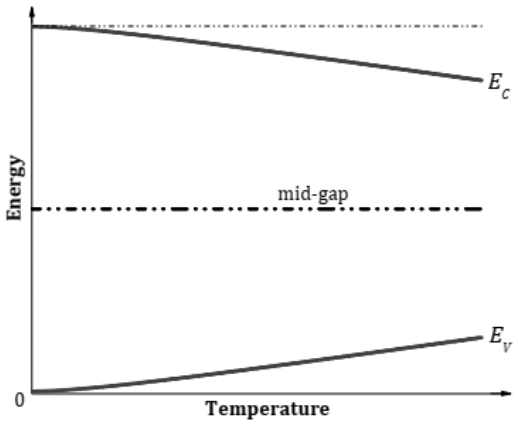

Figure 2.4: Energy band gap versus temperature of a semiconductor [41].

2.3 Thermal equilibrium properties of semiconductors

In this section, the description of some common properties of semiconductor materials like electrical properties, thermal equilibrium concentrations, pure and doped semiconductors, band bending and the energies of the charge carriers and the free charge carrier concentrations will be discussed in detail.

2.3.1 Electrical properties of Gallium antimonide semiconductor

In the world today, there exists the need for advances in high speed, energy-efficient electronic applications. In the fields of lasers, transistors, and thermophotovoltaic systems, one potential improvement that is currently being explored is the use of gallium antimonide (GaSb), an III-V semiconducting material that has interesting electrical properties [43].

Among the III-V binary semiconductors, gallium antimonide has many of its interesting properties directly associated with its very low effective electron mass and high electron mobility of $300\text{cm}^2\text{V}^{-1}\text{s}^{-1}$ and high hole mobility of $1000\text{cm}^2\text{V}^{-1}\text{s}^{-1}$ with the concentration equal to $1.5x10^{15}$ cm $^{-3}$ at room temperature i.e. 300K. The room temperature refractive index of gallium antimonide is 3.8 and its static dielectric constant is 15.7 whereas at high frequency it is 14.4 and also a Debye temperature of 266K [44, 45].

2.3.2 Thermal equilibrium charge carriers

The density of state function in the conduction and valence of band of a semiconductor provided that free electron mass either the electrons density of state effective mass (m_p) in the valence band of electrons density of state effective mass (m_n) in the conduction band. Effective masses for holes and electrons of states of GaSb is given in [46].

$$m_p^* = 0.35 m_n \tag{2-3}$$

and the effective mass of electron is

$$m_n^* = 0.047 m_n \tag{2-4}$$

The total density of electrons in the semiconductor is obtained from Eqn. (2-3) and Fermi energy as:

$$n_0 = N_C exp\left(-\frac{E_C - E_F}{k_B T}\right), in\ the\ conduction\ band \tag{2-5}$$

The total density of holes in the semiconductor is obtained from Eqn. (2-3) and Fermi energy as:

$$p_0 = N_v exp\left(-\frac{E_F - E_V}{k_B T}\right), in\ the\ valence\ band \tag{2-6}$$

where, N_C *and* N_V are the effective density of conduction band states and the effective density of the valence band states respectively, which are the expressions for the equilibrium holes density in the valence band and electrons density in the conduction band [47].

$$N_C = \left(\frac{2\pi m_n^* K_B T}{h^2}\right)^{3/2}, \qquad N_V = \left(\frac{2\pi m_p^* K_B T}{h^2}\right)^{3/2} \tag{2-7}$$

2.3.3 Intrinsic Semiconductors

An intrinsic semiconductor is a pure semiconductor having no impurities. In an intrinsic semiconductor, the numbers of excited electrons and holes are equal, i.e., $n = p$ as shown in figure 2-4. In pure semiconductors, free carriers are generated exclusively by the process of electron-hole-pair described above. Therefore, the concentration of electrons in the equilibrium equals the concentration of holes. Such semiconductor is called an intrinsic semiconductor [48]. A semiconductor may be considered as an intrinsic semiconductor if its thermally generated carrier density represented by n_i is much larger than the background doping or residual impurity densities. For an intrinsic semiconductor the Fermi level, is equal to the intrinsic level energy, in the semiconductor from Eqn. (2-5) and Eqn. (2-6)[49]

$$n_i = N_C\, exp\left(-\frac{E_C - E_i}{k_B T}\right) = N_V\, exp\left(-\frac{E_i - E_V}{k_B T}\right) \tag{2-8}$$

where an intrinsic energy is given by

$$E_i = \left(\frac{E_C + E_V}{2}\right) + \frac{3}{4}(k_B T) ln\left(\frac{m_p^*}{m_n^*}\right) \tag{2-9}$$

As soon as we have known m_p^* , m_n^* and E_g at a given temperature, it is more sophisticated to easily calculate the values of n_i and E_i using Eqn. (2-9) into(2-8).

In the non-degenerate semiconductor case:

$$n_i = \sqrt{n_0 p_0} = \sqrt{N_C N_V} exp\left(\frac{-E_g}{2k_B T}\right) \tag{2-10}$$

Eqn. (2-10) is called the law of mass action. Which indicates that if $m_p^* = m_n^*$ or $T = 0$. the Fermi level in an intrinsic semiconductor is positioned at mid-gap [50, 51].

2.3.4 Extrinsic Semiconductors

A semiconductor in which doping has been introduced, thus changing the relative number and type of free charge carriers, is called an extrinsic semiconductor. An extrinsic semiconductor is a semiconductor in which conduction electrons are the majority carriers is an n-type semiconductor and it is said to be its band diagram are illustrated in and also, it a semiconductor in which the holes are the majority charge carriers is a p-type semiconductor. In extrinsic semiconductors, the dopant concentration N_d is much larger than the thermally generated electron-hole pairs n_i and is temperature independent at room temperature. Adding donor or acceptor impurity atoms into semiconductor will change the distribution of electrons and holes in the material, and as a result, the Fermi energy will change and eliminating N_C and N_V among Eqns. (2-5), (2-6) and (2-8) [52].

The law of mass action Eqn. (2-10) allows one to calculate the minority carrier density in an extrinsic semiconductor when the majority carrier density is known:

$$Minority\ carrier\ density = \begin{cases} \frac{n_i^2}{p_0}, & for\ P-type\ \ material \\ \\ \frac{n_i^2}{n_0}, & for\ N-type\ material \end{cases} \tag{2-11}$$

The thermal equilibrium extrinsic Fermi-level position can also be described from Eqns. (2-5) and (2-6) in terms of E_i and the thermal equilibrium carrier concentrations as: [53].

$$E_F = E_i - (k_B T)\, ln\left(\frac{p_0}{n_i}\right) = E_i + (k_B T)\, ln\left(\frac{n_0}{n_i}\right) \qquad (2\text{-}12)$$

As the charge carrier concentrations change, the position of the extrinsic Fermi energy level varies within the bandgap until the system reaches thermal equilibrium. Relations in Eqns. (2-12) shows that E_F lies above E_i for n-type material ($n_i > p_0$) and below E_i for p-type material ($n_i < p_0$) [54]. Fermi energy level, and the letters i, n and p indicate intrinsic, n-type and p-type material respectively. E_c and E_v are the edges of the conduction and valence bands.

By adding some impurities to a semiconductor its electrical properties can be changed. A semiconductor in which the concentration of electrons is greater than the concentration of the holes is said to be an extrinsic n-type semiconductor. The concentration of electrons in silicon and germanium (which are tetravalent elements, i.e., have four-valence electrons) can be increased by doping with pentavalent elements such as phosphorus, and arsenic. These elements have five valence electrons, but only four are necessary to form a covalent bond with the host semiconductor [55].

A P-type semiconductor is a semiconductor in which hole concentration is higher than electron concentration, which is obtained by adding acceptor impurities. In silicon and germanium, acceptors are usually tri-valence elements, such as Boron. since these elements have only three valence electrons, one is missing to complete covalent bonds with host semiconductor atoms. Therefore, such an atom will bind an electron that would otherwise jump from the valence band into the conduction band, thus preventing the formation of electron hole-pair. Acceptor impurities thus introduce energy states within the energy gap, very close to the valence band. Since ionization energies of typical donors and acceptors impurities are rather small (10mev to 50mev), at room temperature (T=300K) almost all impurities are ionized [56].

2.3.5 Statistics of Donors and Acceptors

The concept of donors and acceptors is expressed in the energy band model in the following manner. Although less important than E_C *and* E_V, two other energy levels are existing in the

energy band diagram, namely, the donor energy level E_d and the acceptor energy level E_a as in Figure 2.5.

Recall that it takes the donor ionization energy (about 50meV) to free the extra electron from the donor atom into a conduction electron. Therefore, the donor electron, before the electron is freed, must occupy a state at about 50meV below E_C. That is to say, $E_C - E_d$ is the donor ionization energy. Similarly, $E_a - E_V$ is the acceptor ionization energy (i.e., the energy it takes for an acceptor atom to receive an extra electron from the valence band, creating a hole there). Acceptor and donor levels with small ionization energies, doped to an element or to a compound are termed to at shallow levels [58].

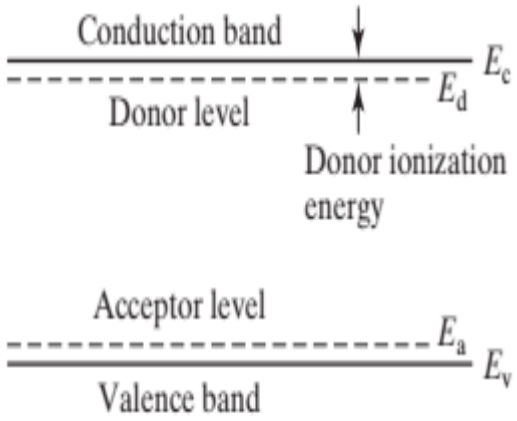

Figure 2.5: Schematic diagram of shallow donor levels and shallow acceptor levels [57].

Recent studies conducted at low-level temperature showed Fe doped by GaSb formed the shallow acceptor level with the ionization energy of 23±2mev. However, the transition metal impurities in GaSb are usually much shallower than that of Fe. For instance, the acceptor level of Mn in GaSb is only 18 meV). The density of electrons in a shallow-donor state is obtained by [59].

$$n_d = \frac{N_d}{1 + \frac{1}{g_d}\exp\left(\frac{E_d - E_F}{k_B T}\right)} \tag{2-13}$$

where n_d, is the density of electrons occupying the donor level, N_d is the concentration of donor atoms, E_d is the energy of donor level and $g_d = 2$ is the donor-site degeneracy factor. The concentration of ionized donors N_d^+ is then:

$$N_d^+ = N_d - n_d = \frac{N_d}{1 + g_d exp\left(\frac{E_F - E_d}{k_B T}\right)} = \frac{N_d}{1 + 2exp\left(\frac{E_F - E_d}{k_B T}\right)} \tag{2-14}$$

When a single ionizable donor captures an electron it becomes neutral, and when it releases an electron, it becomes positively charged. Using the same analysis for the concentration of ionized acceptors N_a^- we have: [50]

$$N_a^- = N_a - p_a = \frac{N_a}{1 + g_a \exp\left(\frac{E_a - E_F}{k_B T}\right)} = \frac{N_a}{1 + 4 \exp\left(\frac{E_a - E_F}{k_B T}\right)} \quad (2\text{-}15)$$

where p_a is the density of holes bound to acceptors, N_a is the concentration of acceptor atoms, E_a is the energy of the acceptor level relative to the valence band, N_a^- is the concentration of ionized acceptor atoms and $g_a = 2xg_d = 4$ is the acceptor site degeneracy factor. When free electron-hole pairs annihilate through recombination, the free carrier concentrations in the conduction and valence bands adjust for the intrinsic semiconductor to $n_0 = p_0 = n_i$. For the extrinsic semiconductors this takes the form:

$$n_0 = N_d^+ + \Re - n_R, and\ P_0 = N_a^- + \Re - n_R \quad (2\text{-}16)$$

where n_R is the concentration of the total electron-hole pairs being annihilated each other after the donors and the acceptors are being ionized, $\Re$ is the concentration of electron-hole pairs thermally generated from band to band, N_a^- and N_d^+ are the densities of free electrons and holes contributed by the donor and the acceptor levels to the respective conduction and valence bands [61].

2.3.6 Charge Neutrality Condition

In thermal equilibrium, the semiconductor crystal is electrically neutral. The electrons are distributed among the various energy states, creating negative and positive charges, but the net charge density is zero. This means the concentration of positive charges is equal to the concentration of negative charges. The positive charges include holes (p) and donors (N_d). The negative charges include electrons (n) and acceptors (N_a). This charge-neutrality condition is used to determine the thermal-equilibrium electron and hole concentrations as a function of the impurity doping concentration. A compensated semiconductor (one that contains both donor and acceptor impurity atoms in the same region) is favored to determine the electron and hole concentrations as a function of the donor and acceptor concentrations [62].

A compensated semiconductor can be formed, for example, by diffusing acceptor impurities into an n-type material or by diffusing donor impurities into a p-type material. An n-type

compensated semiconductor occurs when $N_d > N_a$, and a p-type compensated semiconductor occurs when $N_a > N_d$.

If $N_a^- = N_d^-$, we have a completely compensated semiconductor that shows the characteristics of an intrinsic material. Compensated semiconductors are created quite naturally during device fabrication. The charge neutrality condition is expressed by equating the density of negative charges to the density of positive charges. We then have [63].

$$n_0 + N_a^- = p_0 + N_d^+ \tag{2-17}$$

where n_0 and p_0 are the thermal-equilibrium concentrations of electrons and holes in the conduction band and valence band, respectively. The parameter n_d is the concentration of electrons in the donor energy states, so $N_d^+ = N_d - n_d$ is the concentration of positively charged donor states. Similarly, $p_a$is the concentration of holes in the acceptor states, so $N_a^- = N_a - p_a$ is the concentration of negatively charged acceptor states. We have expressions for $n_0,\ p_0,\ n_d\ and\ p_a$ in terms of the Fermi energy and temperature.

If we assume complete ionization, n_d and p_a are both zero, and Eqn. (2-17) becomes:

$$n_0 + N_a^- = p_0 + (N_d^- - n_d) \tag{2-18}$$

If we express n_0 as $\frac{n_i^2}{p_0}$ from the law of mass action, then Eqn. (2-18) by the application of the law of mass action becomes:

$$\frac{n_i^2}{p_0} + N_a^- = p_0 + N_d^- \tag{2-19}$$

The hole concentration p_0 can be determined using the quadratic formula:

$$p_0^2 - (N_a^- - N_d^-)p_0 - n_i^2 = 0 \tag{2-20}$$

Solving the quadratic formula, the hole concentration will be given by

$$p_0 = \frac{(N_a^- - N_d^-)}{2} + \sqrt{\left(\frac{N_a^- - N_d^-}{2}\right)^2 + n_i^2} \tag{2-21}$$

This equation is used to compute the thermal equilibrium majority carrier hole concentration in a P-type semiconductor, or when $N_a^- \gg N_d^-$. This equation also applies for $N_d^- = 0$. The density of the ionized impurities at the donor and acceptors are given by:

$$N_a^- = N_V \exp\left(\frac{E_V - E_F}{k_B T}\right) \qquad \text{and} \qquad N_a^- = \frac{N_a}{1 + g_a \exp\left(\frac{E_a - E_F}{k_B T}\right)} \tag{2-22}$$

The density of the ionized impurities at the donor and acceptors are given by:

$$N_d^+ = \frac{N_d}{1 + 2\exp\left(\frac{E_F - E_d}{k_B T}\right)} \qquad \text{and} \qquad N_a^- = \frac{N_a}{1 + 4\exp\left(\frac{E_a - E_F}{k_B T}\right)}. \tag{2-23}$$

The law of mass action Eqn. (2-10) along with Eqn. (2-19) yields:

$$p_0 = \frac{N_a^- - N_d^+}{2} + \sqrt{n_i^2 + \left(\frac{N_a^- - N_d^+}{2}\right)^2}, \quad n_0 = \frac{N_d^+ - N_a^-}{2} + \sqrt{n_i^2 + \left(\frac{N_d^+ - N_a^-}{2}\right)^2} \tag{2-24}$$

The ionized acceptor concentration applied in this thesis is expressed in terms of the acceptor chemical potential ($E_{\mu a}$). In semiconductor physics, the term Fermi level is a material property which is often used instead of chemical potential. Chemical potential is temperature-dependent whereas, the Fermi level is temperature independent. Equating the right and the left-hand sides of Eqn. (2-22) and solving for the Chemical potential yields:

$$E_{\mu a} = E_a - k_B T \ln\left(\frac{N_V}{2g_a}\left[-1 + \sqrt{1 + 4g_a \frac{N_a}{N_V}\exp\left(\frac{\Delta E_a}{k_B T}\right)}\right]\right). \tag{2-25}$$

and the solved ionized impurities at acceptors are given by:

$$N_a^- = \frac{N_V}{2g_a}\left(-1 + \sqrt{1 + 4g_a \frac{N_a}{N_V}}\right)\exp\left(\frac{\Delta E_a}{k_B T}\right). \tag{2-26}$$

The majority carrier density or the holes, p_0 in an extrinsic semiconductor for very high acceptor impurity concentration $N_a^- \gg N_d^+$ Eqn. (2-23) maybe reduced to:

$$p_0 = \frac{N_a^-}{2} + \sqrt{n_i^2 + \left(\frac{N_a^-}{2}\right)^2} \approx N_a^-. \tag{2-27}$$

The law of mass action, Eqn. (2-10) allows one to calculate the minority carrier density in an extrinsic semiconductor when the majority carrier density is known:

$$n_0 = \frac{n_i^2}{p_0} \tag{2-28}$$

2.4 Energy of free carriers

Electron's energies increase upward, while the hole's energies increase downward in the energy band diagram. The kinetic energy (E_K) of a carrier is equal to the energy difference between the carrier's level in a band and the band edge may be given as:

$$E_{kn} = E - E_C\,, \quad for\ electrons \quad and \quad E_{kp} = E_V - E\,, \qquad for\ holes \tag{2-29}$$

Figure 2.6 Illustrates the kinetic energy and the potential energies of an electron in the conduction band; and the upward increase of electron energy and the downward increase of the hole energy.

The energy supplied to excite an at-rest valence band electron from E_V to E_C is totally used up in the excitation process. The $E = E_C$ electron and $E = E_V$ hole thereby created are therefore at rest. The kinetic and potential energies of an electron in the conduction band; and the upward increase of electron energy and the downward increase of the hole energy. E_C represents the electron potential energy:

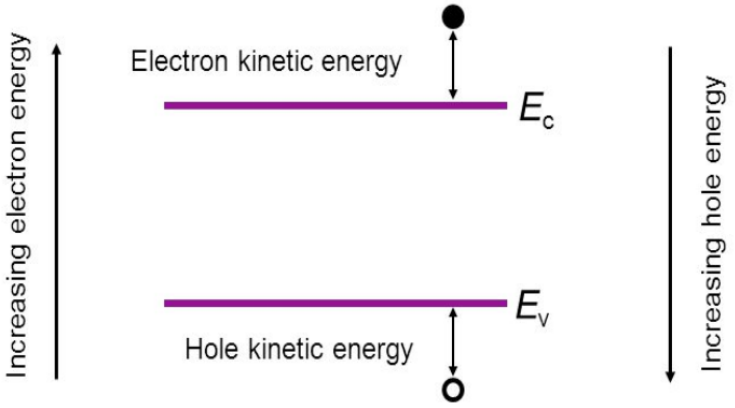

Figure 2.6: The kinetic and potential energies of an electron in the conduction band [32].

$$P.E = E_C - E_{refernce} \tag{2-30}$$

Electron or hole carrier energies are thus logically associated with the kinetic energy. Supposing the electron kinetic energy is E_{kn} and its potential energy is U_n then their sum is equal to the total energy (E).

$$E = E_{kn} + U_n \tag{2-31}$$

The electron potential energy as pictured in Figure 2.6 must be equal to the energy difference between the conduction band edge (E_C) and the reference energy E_0.

$$U_n = E_C - E_0 \tag{2-32}$$

The electron potential energy (and hence the total energy) is, of course, arbitrary to within a constant, and the position-independent reference energy, E_0, maybe chosen to be any convenient value.

2.5 The Band Bending

When looking at a band diagram, the electron energy band in a material can bend up or down in the depletion region. This effect is known as band bending. Band bending refers to the local changes in the energy of a semiconductor's band structure in the depletion region, due to charge effects. Band bending occurs when an electric field is applied to a semiconductor. When there isn't an electric field being applied, the energy bands are not a function of position. Therefore, when an electric field is applied, energy is being supplied to the carriers in the material. Where band bending has occurred, we can measure the energy being given to the electrons or holes by taking a reference energy and measuring the distance between it and the energy the carrier is positioned at [64].

Band bending also occurs while the conduction and valence bands vary with respect to position. Combining the diagram band bending and the relation between U_n *and* E_C Eqn. (2-32), it is possible to deduce, by inspection, the general form of the electrostatic variables inside the material. From the earlier concept of physics, the potential energy of a negatively charged particle is related to the electrostatic potential V at a given point in the material by:

$$U_n(x) = -eV(x) \tag{2-33}$$

Thus, taking into account Eqn. (2-32) along with Eqn. (2-33), yields:

$$V(x) = -\frac{1}{e}(E_C - E_0) \tag{2-34}$$

There is an electric potential V inside the device is given by:

$$\varepsilon = -\nabla \mathrm{V} \tag{2-35}$$

For one dimensional along x-axis:

$$\varepsilon = -\frac{dV}{dx} \tag{2-36}$$

Upon substituting Eqn. (2-34) into Eqn. (2-36), we get:

$$\varepsilon = \frac{1}{e}\frac{dE_C}{dx}, \qquad E_0 = constant \tag{2-37}$$

and

$$\varepsilon = \frac{1}{e}\frac{dE_V}{dx}, \qquad E_g = constant \tag{2-38}$$

The volume charge density in the material is also given from Poisson's rule as:

$$\bar{N}(x) = \epsilon \frac{d\varepsilon}{dx} = -\epsilon \frac{d^2V(x)}{dx^2} \tag{2-39}$$

If the field is applied in the region of width X in the material directing from left to right, the position dependence of the conduction band edge and the corresponding potential in the field region of the material are given as:

$$E_C(x) = E_{C0} + e\int_0^X \varepsilon(x)dx, \quad V(x) = V_0 - e\int_0^X \varepsilon(x)dx, \tag{2-40}$$

where E_{C0} and V_0 are the conduction band edge and the corresponding potential at $x = 0$. The primary principle underlying band bending inside a semiconductor is space charge (imbalance in charge neutrality). The band bending that occurs inside the depletion regions implies the presence of an electric field and a corresponding electrostatic potential. But the Fermi level in equilibrium is flat and constant throughout the device [65].

For simplicity, the semiconductor will be considered as a uniformly doped, semi-infinite crystal in thermal equilibrium. Accordingly, the semiconductor surface is defined by a plane located at $x = 0$ perpendicular to the X-axis. Hence, the bulk of the semiconductor is characterized by positive values of x. Naturally, an electrostatic surface potential, V is defined directly from Poisson's equation: [66].

$$\frac{d^2V}{dx^2} = \frac{-N_{net}(x)}{\epsilon} \tag{2-41}$$

Here, $N_{net}(x)$ is the net charge density and ϵ_S is the permittivity of the material. Clearly, $N_{net}(x)$ can be written as just the sum of contributions from mobile carriers and ionized dopant atoms:

$$N_{net}(x) \ = e[p_0(x) - n_0(x) + N_d^+ - N_a^+] \tag{2-42}$$

Of course, in contrast to the simple case of bulk semiconductor, carrier concentrations near the surface are explicit functions of x; however, $N_d^+ \ and \ N_a^+$ remain independent of x due to the assumption of uniform doping. It follows from the fundamental definition previously given in Eqn. (2-6) for position dependence of majority carrier concentration as a function of depth becomes:

$$p_0(x) = N_V exp\left(-\frac{E_F - E_V(x)}{k_B T}\right) = N_V exp\left(-\frac{E_F - (E_{V0} - \Delta E)}{k_B T}\right) \tag{2-43}$$

where the term $E_V(x)$ is position-dependent valence band energy, E_{V0} is the initial valence band energy at its reference position and the term ΔE is the change in energy between E_{V0} and $E_V(x)$. Thus, the above equation of majority carrier concentration would become:

$$p_0(x) = p_0 exp\left(\frac{-\Delta E}{k_B T}\right) \tag{2-44}$$

In a similar technique, one can accomplish the position dependence of minority carrier concentration from Eqns. (2-10) and (2-11) as:

$$n_0(x) = n_0 exp\left(\frac{\Delta E}{k_B T}\right) \tag{2-45}$$

Hence for p-type semiconductor with $N_a^- = p_0 + n_i \approx p_0,\ and\ N_a^- \gg N_d^+$ the net charge density Eqn. (2-28) in the depletion region will be computed as:

$$N_{net}(x) = e[p_0 - n_0 + n_0(x) - p_0(x)] \tag{2-46}$$

Insertion of the values of Eqn. (2-44) and (2-31) into Eqn. (2-46) provides:

$$N_{net}(x) = e\left(p_0 + n_0 exp\left(\frac{\Delta E}{k_B T}\right)\right)\left(1 - exp\left(\frac{-\Delta E}{k_B T}\right)\right) \tag{2-47}$$

2.6 The near-surface region at thermal equilibrium

The bulk of most isolated III-V semiconductors have three various regions of different carrier concentrations. This consists of a neutral region (with high thermal equilibrium majority carrier concentration), followed by a transition layer (with decreasing thermal equilibrium majority carrier concentration in moving towards the surface), and a depleted surface region of very low thermal equilibrium majority carrier concentration [67].

In semiconductor physics, the depletion region, also called depletion layer, depletion zone, junction region, space charge region or space charge layer, is an insulating region within a conductive, doped semiconductor material where the mobile charge carriers have been diffused away, or have been forced away by an electric field. The only elements left in the depletion region are ionized donor or acceptor impurities. The depletion region is so named because it is formed from a conducting region by removal of all free charge carriers, leaving none to carry a current. In the depletion region of a semiconductor, the free carrier concentration is very small as compared to the bulk [68].

The width of the total depletion layer b_1, between the surface and the neutral region is given by the sum of the width of the highly depleted layer (b_s) and the width of the transition region (b_δ) between the highly depleted region and the quasi-neutral region [69].

$$b_1 = b_s + b_\delta \tag{2-48}$$

The position dependence of electric field strength depth x below the surface in the depletion layer can be determined by applying Gauss's law to both the surface and the depth x below the surface as:

$$\varepsilon(x) = \frac{1}{\epsilon}[\sigma + x\bar{N}(x)] \tag{2-49}$$

where $\bar{N}(x)$ the average volume charge density in the region of depth x from the surface and σ is the surface charge density. The average net volume charge density in the region of depth x below the surface $\bar{N}(x)$ can be determined using Eqn. (2-47) as:

$$\bar{N}(x) = -eN_a^- \left[1 + \frac{k_B T}{E_S - E(x)} exp\left(\frac{-E_S}{k_B T}\right)\left[1 - exp\left(\frac{E_S - E(x)}{k_B T}\right)\right]\right] \tag{2-50}$$

where E_S is the band bending at the surface and $E(x)$ is the band bending at depth x.

The charge density near the surface region is evaluated by make use of the concept $E(x) \approx E_S$. Thus, the term $exp\left(\frac{E_S - E(x)}{k_B T}\right)$ will be approximated by the binomial expansion to give rise to $exp\left(\frac{E_S - E(x)}{k_B T}\right) \approx 1 + \frac{E_S - E(x)}{k_B T}$.

Therefore, the charge density near the surface will be given by:

$$\bar{N}_S = -eN_a^- \left[1 - exp\left(\frac{E_S}{k_B T}\right)\right] \tag{2-51}$$

In the transition layer, the charge density will be computed as soon as we replace the energy bending at any depth $E(x)$ by the energy bending at the edge of the transition layer $E_{\delta=}\, k_B T$. Hence, the charge density in the transition layer will be:

$$\bar{N}_\delta = -eN_a^- \left[1 - \frac{k_B T}{E_S - E_\delta}\left[exp\left(\frac{-E_\delta}{k_B T}\right) - exp\left(\frac{-E_S}{k_B T}\right)\right]\right] \tag{2-52}$$

Similarly, the charge density in the entire depletion region (between the surface and the quasi-neutral region) where $E_S \gg E(x)$ or when $E(x) \longrightarrow 0$ can be given from the Eqn. (2-63) by:

$$\bar{N}_1 = -eN_a^- \left[1 - \frac{k_B T}{E_S}\left[1 - exp\left(\frac{-E_S}{k_B T}\right)\right]\right] \tag{2-53}$$

The three charge densities (near-surface, transition layer and the quasi-neutral) and the average charge density can be computed if the room temperature surface Fermi level E_{SF} position is known. Equation that relates the band bending and the Fermi-level position at the surface of a p-type semiconductor.

$$E_S = E_{SF} - E_{BF} \tag{2-54}$$

The Fermi energy in the bulk of a semiconductor is provided by the relation in Eqn. (2-12) stated earlier. Since the electric field $\varepsilon(x)$ and energy bending $E(x)$ are zero at the edge of the quasi-neutral region ($x = b_1$) in Eqns. (2-43) and(2-44), the surface charge density σ can also be described using Eqn. (2-43) as:

$$\sigma \approx -b_1 \bar{N}_1 \left[1 - \frac{k_B T}{E_S}\left[1 - exp\left(\frac{-E_S}{k_B T}\right)\right]\right] \tag{2-55}$$

The electric field strength at depth x below the surface of p-type semiconductor can be found using Eqn. (2-43) as:

$$\varepsilon(x) = \frac{-\bar{N}_1}{\epsilon}\begin{cases} b_1 - x\left(\bar{N}_S \big/ \bar{N}_1\right), near\ surface\ region \\ b_1 - x\left(\bar{N}_\delta \big/ \bar{N}_1\right), \ \ in\ transition\ layer \\ b_1 - x, \ \ near\ quasi-neutral\ region \end{cases} \tag{2-56}$$

Applying relations between the energy and the electric field discussed in the previous subsection to Eqn. (2-43) the energy bending in the depletion layer is hence given by:

$$E(x) = \frac{e\bar{N}_1}{2\epsilon}\begin{cases} \left[(b_1 - x)^2 - \left(1 - \left(\frac{\bar{N}_S}{\bar{N}_1}\right)x^2\right)\right], near\ surface\ region \\ \left[(b_1 - x)^2 - \left(1 - \left(\frac{\bar{N}_\delta}{N_1}\right)x^2\right)\right], in\ transition\ layer \\ [(b_1 - x)^2] \qquad\qquad in\ entire\ depletion\ region \end{cases} \tag{2-57}$$

Hence, the position dependence of the band bending in energy in the entire depletion layer between the surface and the edge of the quasi-neutral region can be approximated in general as [70].

$$E(x) = \frac{e\bar{N}_1}{2k_\infty \epsilon_0}(b_1 - x)^2 \tag{2-58}$$

where $E(x)$ is the band bending at depth x, $\bar{N}_1$is near surface charge density,ϵ is dielectric constant (14.4) and ϵ_0 is permittivity of free space ($8.85x10^{12}\ C^2/Jm$).

The surface band bending which is attained at $x = 0$, in the above relation could given as:

$$E_S = \frac{e\bar{N}_1}{2k_\infty \epsilon_0} b_1^2 \tag{2-59}$$

The width of the depletion region can thus be performed by using the relation:

$$b_1 = \sqrt{\frac{2E_S k_\infty \epsilon_0}{e\bar{N}_1}} \tag{2-60}$$

Similarly at the edge of the transition layer ($x = b_S$) since the energy bending remains unaltered $E(x = b_S) = E_\delta = k_B T = \frac{e\bar{N}_1}{2k_\infty \epsilon_0}(b_1 - b_S)^2 = \frac{e\bar{N}_1}{2k_\infty \epsilon_0} b_\delta^2$, the width of the transition layer will be given by:

$$b_\delta = \sqrt{\frac{2E_\delta k_\infty \epsilon_0}{e\bar{N}_1}} \tag{2-61}$$

At the edge of the quasi-neutral region (where $x = b_1$), the energy band bending vanishes and hence, $E(x = b_1) = 0$.

2.7 Excess Carriers recombination in semiconductors

The generation of excess carriers in a semiconductor may be accomplished by either electrical or optical means. For example, electron-hole pairs are created in a semiconductor when photons with energies exceeding the bandgap energy of the semiconductor are absorbed. The inverse process to the generation of excess carriers in a semiconductor is that of recombination. The annihilation of excess carriers generated by optical or electrical means in a semiconductor may take place via different recombination mechanisms. Depending on the ways in which the energy of an excess carrier is removed during a recombination process, there are three basic recombination mechanisms that are responsible for carrier annihilation in a semiconductor. They are nonradiative recombination (i.e., the multiphoton process), band-to-band radiative recombination, and Auger band-to-band recombination. The electron-hole pair is the fundamental unit of generation and recombination, corresponding to an electron transitioning between the valence band and the conduction band where the generation of electron is a transition from

the valence band to the conduction band and recombination leads to a reverse transition [71].

The first recombination mechanism, known as the nonradiative or multiphoton recombination process, is usually the predominant recombination process for indirect bandgap semiconductors such as silicon and germanium. In this process, recombination is accomplished via a deep-level recombination center in the forbidden gap, and the energy of the excess carriers is released via phonon emission. The second recombination mechanism, band-to-band radiative recombination, is usually the predominant process occurring indirect bandgap semiconductors such as GaAs and InP. In this case, the band-to-band recombination of electron-hole pairs is accompanied by the emission of a photon [72].

Auger band-to-band recombination is usually the predominant recombination process occurring in degenerate semiconductors and small-band-gap semiconductors such as InSb and HgCdTe materials. The Auger recombination process can also become the predominant recombination mechanism under high-injection conditions. Unlike the nonradiative and radiative recombination processes, which are two-particle processes, Auger band-to-band recombination is a three-particle process, which involves two electrons and one hole for n-type semiconductors, or one electron and two holes for p-type semiconductors.

For an n-type semiconductor, Auger recombination is accomplished first via electron-electron collisions in the conduction band, and followed by electron-hole recombination in the valence band [73].

2.7.1 The Radiative recombination mechanism

The radiative recombination is a fundamental band -to-band process which determines the electronic band structure of a semiconductor. The role of radiative mechanism in the detection of IR radiation has been recently critically re-examined by Humphreys.

2.7.2 The Auger recombination mechanism

The Auger mechanism dominates generation and recombination processes in high quality and small bandgap semiconductor. The band-to-band Auger effects are classified in several processes according to related bands. Auger recombination mechanisms are possible in a semiconductor with a single conduction band and heavy, light-hole and Split off valence

bands. The Auger recombination mechanism is typically observed in both direct and indirect band-gap semiconductors when either the doping density or the excess carrier density is very high [74].

2.7.3 The Radiative excess carrier lifetime

The average timing between the creation and the disappearing of an electron-hole pair is termed as lifetime. The lifetime varies from nanoseconds to several microseconds depending upon the various factors such as shape, size, crystal structure of the semiconductor material. The radiative excess carrier lifetime is constant at low injection, but then decreases and continues to decrease as the injection level increases. Radiative recombination is typically the dominant recombination process indirect bandgap semiconductors under low injection level, it is considered to be small or even negligible compared to other recombination processes in indirect semiconductors. Radiation which is presumably due to the recombination of free electrons and holes has been observed in gallium antimonide. The radiative lifetime is inversely proportional to the total concentration of free carriers under all circumstances [75].

The total recombination rate R is directly proportional to the product of the concentration of electrons n available in the conduction band and the concentration of holes p available in the valence band:

$$R = C_R np \tag{2-62}$$

provided that the excess carrier concentration hole and electron are given by:

$$p = p_0 + \delta p, \qquad and \qquad n_0 + \delta n \tag{2-63}$$

In thermal equilibrium, the rate of recombination is equal to the rate of thermal generation, which can be expressed by:

$$R_0 = C_R p_0 n_0 = C_R n_i^2 \tag{2-64}$$

where C_R *is* the rate of radiative capture probability derived from the optical absorption process by using the principles of detailed balance and values of C_R for narrow bandgap semiconductors as:

$$C_R = \pi\sqrt{k_\infty}\left(\frac{m_n}{m_n^* + m_p^*}\frac{300}{T}\right)^{3/2}\left(1 + \frac{m_n}{m_n^*} + \frac{m_p}{m_p^*}\right)\left[E_g^2 + 3E_g k_B T + 3.75k_B^2 T^2\right] \quad (2\text{-}65)$$

The net recombination rate is obtained by solving Eqns. (2-58), (2-59) and (2-60) result yields:

$$U = R - R_0 = C_R \delta n(p_0 + n_0 + \delta n) \quad (2\text{-}66)$$

The radiative lifetime, τ_R due to the recombination is obtained by solving by Eqn. (2-62) which yields:

$$\tau_R = \frac{\delta n}{U} = \frac{1}{C_R(p_0 + n_0 + \delta n)} = \frac{\tau_{R0}}{1 + C_R\tau_{R0}\delta n} \quad (2\text{-}67)$$

where

$$\tau_{R0} = \frac{1}{C_R(p_0 + n_0)} \quad (2\text{-}68)$$

From Eqn.(2-67) it is noted that τ_R is inversely proportional to the majority carrier density p_0. Upon substituting the steady-state generation relation $\delta n = G_0\tau_R$ into Eqn. (2-67), the radiative excess carrier lifetime takes the form:

$$\tau_R = \frac{2\tau_k\tau_{R0}}{\tau_{R0} + \tau_k} \quad (2\text{-}69)$$

where τ_k is the time constant given by:

$$\tau_k = \frac{\tau_{R0}}{\sqrt{1 + 4C_R G_0 \tau_{R0}^2}} \quad (2\text{-}70)$$

Under low injection conditions, $\delta n \ll p_0, n_0$, Eqn. (2-43) can be simplified to:

$$\tau_k = \tau_R = \tau_{R0} = \frac{1}{C_R(p_0 + n_0)} \quad (2\text{-}71)$$

2.7.4 The Auger excess carrier lifetime

Similar to the radiative lifetime, the Auger lifetime is independent of any impurity density. Auger recombination is the ultimate recombination mechanism for devices operating at very high injection or at very high doping densities. It is also the dominant recombination mechanism for narrow band-gap semiconductors. Radiative recombination can also occur through intermediate energy levels. When EHP recombine radiatively through intermediate levels, photons are generally emitted for only one of the transitions [76].

The auger recombination is viewed as a triple interaction where a conduction band electron and a valence band hole recombine with excess energy transferred to the third free electron or hole.

$$R_{eeh} = C_{na}n^2p, \quad R_{ehh} = C_{pa}p^2n \tag{2-72}$$

where the terms R is the Auger recombination rate, p the is free carrier concentration of hole and n is the free carrier concentration of electron after some time, the total recombination mechanism rate and its lifetime is given as:

$$R_A = R_{eeh} + R_{ehh} = C_{na}n^2p + C_{pa}p^2n \tag{2-73}$$

Auger recombination rate for equilibrium conditions, R_0 is then given by:

$$R_0 = C_{na}n_0^2p_0 + C_{pa}p_0^2n_0 \tag{2-74}$$

The hole and electron free carrier concentrations are expressed as: $p_0 = n_0 + \delta p, \ \ and\ n_0 = n_0 + \delta n$. Incorporation of Eqn. (2-74) in to the term in Eqn. (2-73) above yields:

$$U_A = \delta n(C_{pa}(p_0^2 + 2n_i^2) + C_{na}(n_0^2 + 2n_i^2)) + \ \delta n^2(C_{pa}(2p_0 + n_0) + C_{na}(2n_0 + p_0)) + \delta n^3(C_{pa} + C_{na}) \tag{2-75}$$

The simplified form of the Auger recombination rate, U_A for photo-generated carriers in Eqn. (2-73)becomes:

$$U_A \approx \frac{\delta n}{\tau_{A0}} + k_A\delta n^2 + C_A\delta n^3 \tag{2-76}$$

and the Auger recombination lifetime for excess carriers is then given by:

$$\tau_A = \frac{\tau_{A0}}{1 + \tau_{A0}(k_A\delta n + C_A\delta n^2)} \tag{2-77}$$

where

$$\tau_{A0} = \frac{1}{C_{pa}(p_0^2 + 2n_i^2) + C_{na}(n_0^2 + 2n_i^2)}, \qquad C_A = C_{pa} + C_{na} \tag{2-78}$$

and

$$k_A = C_{pa}(2p_0 + n_0) + C_{na}(2n_0 + p_0) \tag{2-79}$$

For narrow bandgap p-type semiconductors, Auger recombination due to valence band splitting is favored, $C_{pa} \gg C_{na}$, so that, $\tau_{A0} \approx \frac{1}{C_{pa}p_0^2}$, $k_A \approx 2C_{pa}p_0$, and $C_A \approx C_{pa}$. Therefore, the auger recombination lifetime under low injection level conditions ($\delta n = \delta p \ll p_0, n_0$) will be given by the relation [23].

$$\tau_A = \frac{1}{C_{pa}(p_0^2 + 2n_i^2) + C_{na}(n_0^2 + 2n_i^2)} \tag{2-80}$$

2.7.5 The Effective carrier lifetime

The effective excess minority carrier lifetime in the entire sample (*i.e.* bulk plus surface recombination) is determined by considering the sum of all the recombination rates through all the recombination channels discussed above. This is the sum of the bulk recombination rate and the surface excess minority carrier recombination rate [58]. The recombination lifetime in the bulk determined by the recombination's mechanism radiative and Auger recombination according to the relationship (2-71) and (2-80).

The effective lifetime for both recombination mechanisms in the simplified form of the well-known radiative (τ_R) and Auger (τ_A) excess carrier recombination lifetimes are described in terms of the thermal equilibrium carrier concentration p_o and n_0 for p-type bulk material as [25]. From the combination of equation (2-71)and (2-80) we obtained as follows:

$$\frac{1}{\tau_{\text{eff}}} = \frac{1}{\tau_R} + \frac{1}{\tau_A} \qquad \text{or} \qquad \tau_{\text{eff}} = \left(\frac{1}{\tau_R} + \frac{1}{\tau_A}\right)^{-1} \tag{2-81}$$

Chapter 3 : Methodology

For the analysis of the thermal equilibrium properties of the group IIIB-IVB compound semiconductors near the surface and depletion region in this thesis, Gallium antimonide (GaSb) was found to be suitable. This is due to its small and direct bandgap, very high carrier densities, high mobility, and its very high purity. The majority carrier concentration, p_0 and surface Fermi level position, (E_{SF}) used in the analysis were taken from the simulation of the existing temperature dependence Hall measurements data measured at Nelson Mandela Metropolitan University, South Africa. The minority carrier concentration, n_0 is determined from p_0 and the intrinsic carrier concentration (n_i) using the law of mass action for a specific semiconductor using the relation in Eqn. (2-10). The typical carrier capture coefficients used in the analysis were $C_R = 1.12\text{x}10^{-10}\text{cm}^3\text{s}^{-1}$ for radiative recombination, $C_{pa} = 5x10^{-26}cm^6s^{-1}$and $C_{na} = 5x10^{-29}cm^6s^{-1}$ for Auger holes capture and for Auger electron capture respectively.

The energy bending at the surface, E_S is determined from the surface pinning fermi energy E_{SF} and the Fermi-level position relative to the valence band maximum (VBM) in the bulk for low doping p-type semiconductor by the relation (2-54). Then energy band bending at any depth in the entire depletion region (near the surface, in the transition layer and near quasi-neutral region) were computed by the application of the relation (2-57) and analyzed using the linear graphs for vertical and horizontal axis.

The necessary data for the majority and the minority carrier concentrations versus position (depth below the surface) were collected using Eqns. (2-44) and (2-45) analyzed using a semi-log graph for the vertical axis and linear for the horizontal axis.

The average charge density at any depth in the depletion region was determined by means of Eqn. (2-50) and the net charge density in the depletion region which depends on the thermal equilibrium carrier concentrations and the thermal carrier concentrations as a function of depth in the depletion region was investigated using the Gauss's law depicted in relation (2-47). And the results for both were analyzed using the semi-log for the vertical axis and linear for the horizontal one.

The electric field strength in the three layers of the depletion region namely, the near-surface region, the transition layer, and the near quasi-neutral region was given by the relation in (2-56). The average electric field in the entire depletion region is however, the single graph evaluated by the application of the relation (2-49).

The effective excess carrier lifetimes were determined using the two recombination mechanisms namely, radiative and Auger that are usually dominant in small bandgap semiconductors. The radiative lifetime (τ_R) and Auger lifetime (τ_A) for excess carriers in p-type GaSb material are determined as functions of position and injection level. The theoretical results were analyzed using the thermal equilibrium majority carrier concentration results from Hall Effect measurements along with the relations describing the effective excess carrier lifetimes in the bulk of direct bandgap semiconductor.

The data for the radiative recombination lifetime τ_R was described using Eqn.(2-71) then the auger recombination lifetime using Eqn. (2-80) and finally, the effective carrier lifetime was determined using Eqn. (2-81) by varying the position from the surface ($x = 0$ nm) to the total depletion width ($x = b_1$) in all the cases. The results of the position dependence of the room temperature minority carrier lifetimes $\left(\tau_{Rad},\ \tau_{Aug}\ \text{and}\ \tau_{eff}\right)$ were described using the combinations the semi-log scale for the vertical axis while the horizontal axis was linear.

In the analysis of data, all the necessary data were analyzed and the crucial graphs are sketched using the Microsoft excel and the final graphs in the result section sketched using the origin 8 software.

Chapter 4 : Result and Discussion

4.1 Energy band bending versus position for different doping concentrations.

Figure 4.1 illustrates the room temperature doping level dependence of energy band bending for p-type semiconductor.

To perform the process of plotting the graph first, the position dependence of energy band bending at any depth near the surface depletion layer of GaSb semiconductor is determined using Eqn. (2-58). The horizontal axis represents the depth below the surface whereas, the vertical one is the energy band bending at any location in the space charge region corresponding to the depths. The width of the under-surface depletion layer is also determined using relation in Eqn. (2-60).

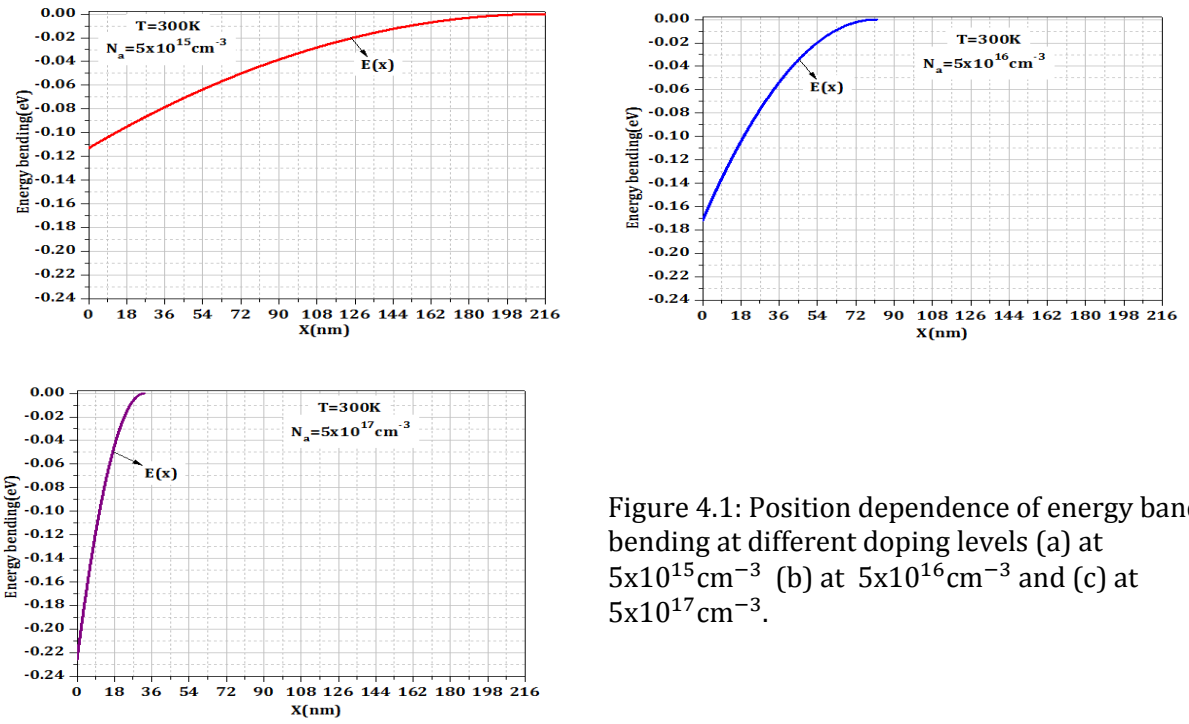

Figure 4.1: Position dependence of energy band bending at different doping levels (a) at $5x10^{15}cm^{-3}$ (b) at $5x10^{16}cm^{-3}$ and (c) at $5x10^{17}cm^{-3}$.

The graph in figure 4.1displays the energy bending is a half parabola which opens downward in order to indicate the energy band bending keeps decreasing as we move from the near-surface region to the quasi-neutral region via the depletion layer. As can be seen in figure 4.1 the energy bending increases with increasing the doping concentration.

The equation is applicable at any depth below the surface in the entire depletion region of the material. We can also infer that there is a very large energy band bending at the surface ($x = 0$) and hence the near-surface region is highly depleted. on the contrary, at the edge of the quasi-neutral region where ($x = b_1$), the band bending becomes zero. Increasing doping causes neutralization to occur sooner. Subsequently, the depletion width decreases as the increase in carrier concentration leads to more recombination of majority carriers. Therefore, high doping leads to a decrease in depletion width. This result is in good agreement with the results received by other researchers [77].

4.2 The majority, minority and intrinsic carrier concentrations versus position at different doping levels.

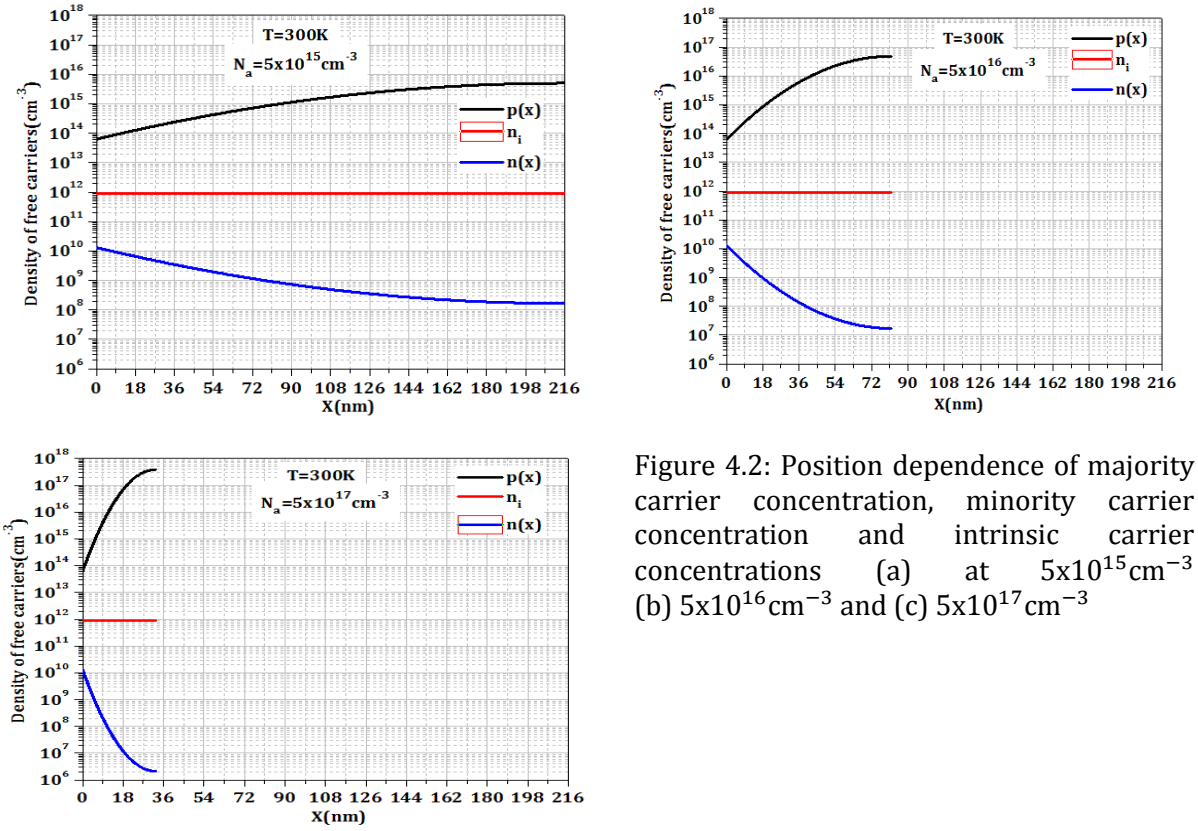

Figure 4.2: Position dependence of majority carrier concentration, minority carrier concentration and intrinsic carrier concentrations (a) at $5x10^{15}cm^{-3}$ (b) $5x10^{16}cm^{-3}$ and (c) $5x10^{17}cm^{-3}$

The expression of the energy bending, $E(x)$ at any location x in the depletion region also enables us to evaluate the thermal equilibrium free carriers concentrations at any point x in the depletion region.

The doping level dependence of majority, minority and intrinsic carrier concentration in the near-surface depletion layer can be determined using Eqns. (2-44) and (2-45) and (2-28) respectively.

Figure 4.2 illustrates the doping level dependence of majority carrier concentration increases as one goes from the near-surface to the deep bulk (quasi-neutral region).
The majority carrier concentration has got its minimum value near the surface where the surface band bending energy is maximum.
Thus, the majority carrier concentration will be minimum. At the edge of the transition layer where the energy band bending is given by $E(x) = E_\delta = k_B T$, the majority carrier concentration gets only 37% of its equilibrium concentration ($0.37p_0$).
Generally speaking, the position dependence of majority carrier concentrations at different doping levels in the near-surface depletion layer of Gallium Antimonide (GaSb) remains minimum in the highly depleted zone slightly increases from the edge of the transition layer on the way to the quasi-neutral region and attains its maximum value p_0 at the edge of the quasi-neutral region.

Figure 4.2 implied by the blue lines indicated the minority carrier concentration versus position at different doping levels. The figures indicate the concentration of minority carries varies in the reverse way to the majority carrier concentrations so as to fulfill the law of mass action which verifies the intrinsic carrier concentration remains constant regardless of variations in doping concentration as in Eqn. (2-10) and Eqn.(2-11). The concentration of minority carrier concentration is maximum at the contact point with the surface, exponentially declines towards the neutral region, attains its equilibrium concentration($n(x) = n_0$) at the edge of the transition layer ($x = b_\delta$) and takes its minimum value at the edge of quasi-neutral region. This result also confirms the results implied by the early researchers done on temperature dependence carrier concentrations under the surface depletion layer of thin-film in Gallium Antimonide semiconductor [77].

4.3 The charge density versus position at different doping concentrations.

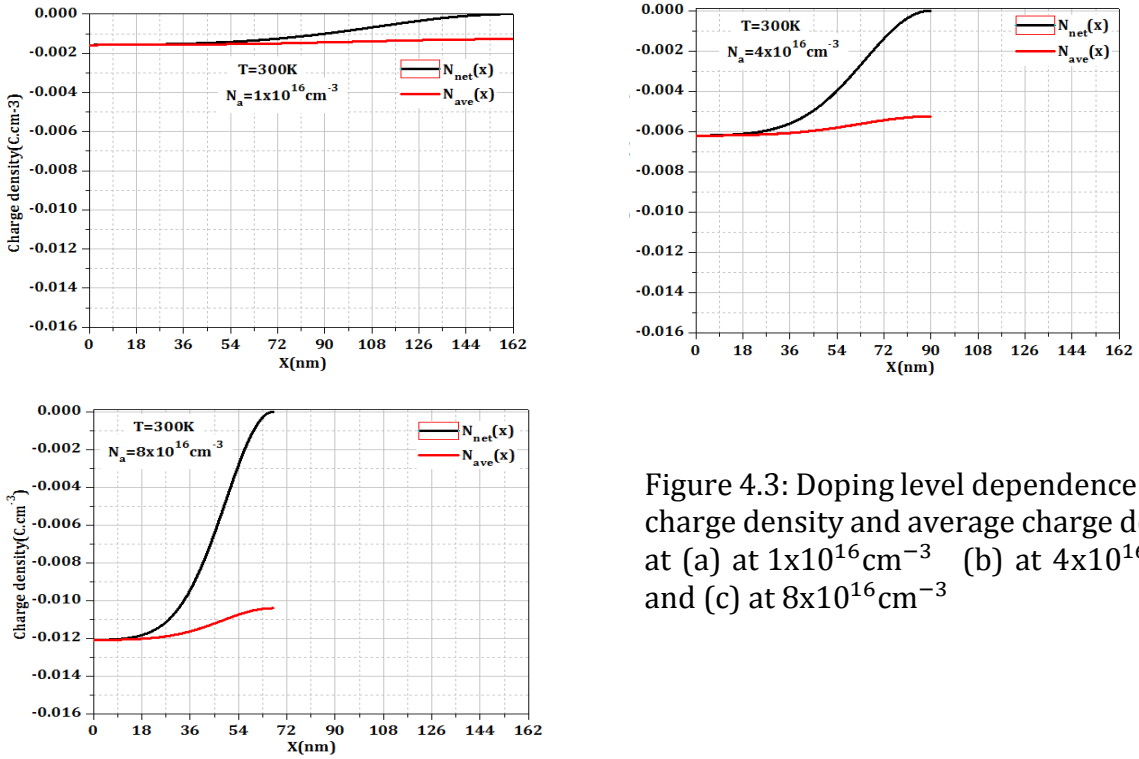

Figure 4.3: Doping level dependence of net charge density and average charge density at (a) at $1x10^{16}cm^{-3}$ (b) at $4x10^{16}cm^{-3}$ and (c) at $8x10^{16}cm^{-3}$

Figure 4-3 indicates the room temperature net and average charge density at different doping levels. The figure is performed using Eqns. (2-47) and (2-50) respectively. The average charge density of free carriers at a low doping level remains constant with only a slight increment. For medium and high doping levels it increases after the near-surface to the quasi-neutral region and remains constant towards the deep bulk region.

Similarly, the net charge density between the surface and any point at depth x below the surface remains constant near-surface region, increasing in the transition region until the edge of the quasi-neutral region and remains constant towards the deep bulk region only with a higher magnitude compared to the average charge density.

The net charge density is greater than the average charge density in the entire region between the highly depleted layer and the near-quasi-neutral regions.

4.4 The electric field intensity versus depth in the depletion region for different doping concentrations

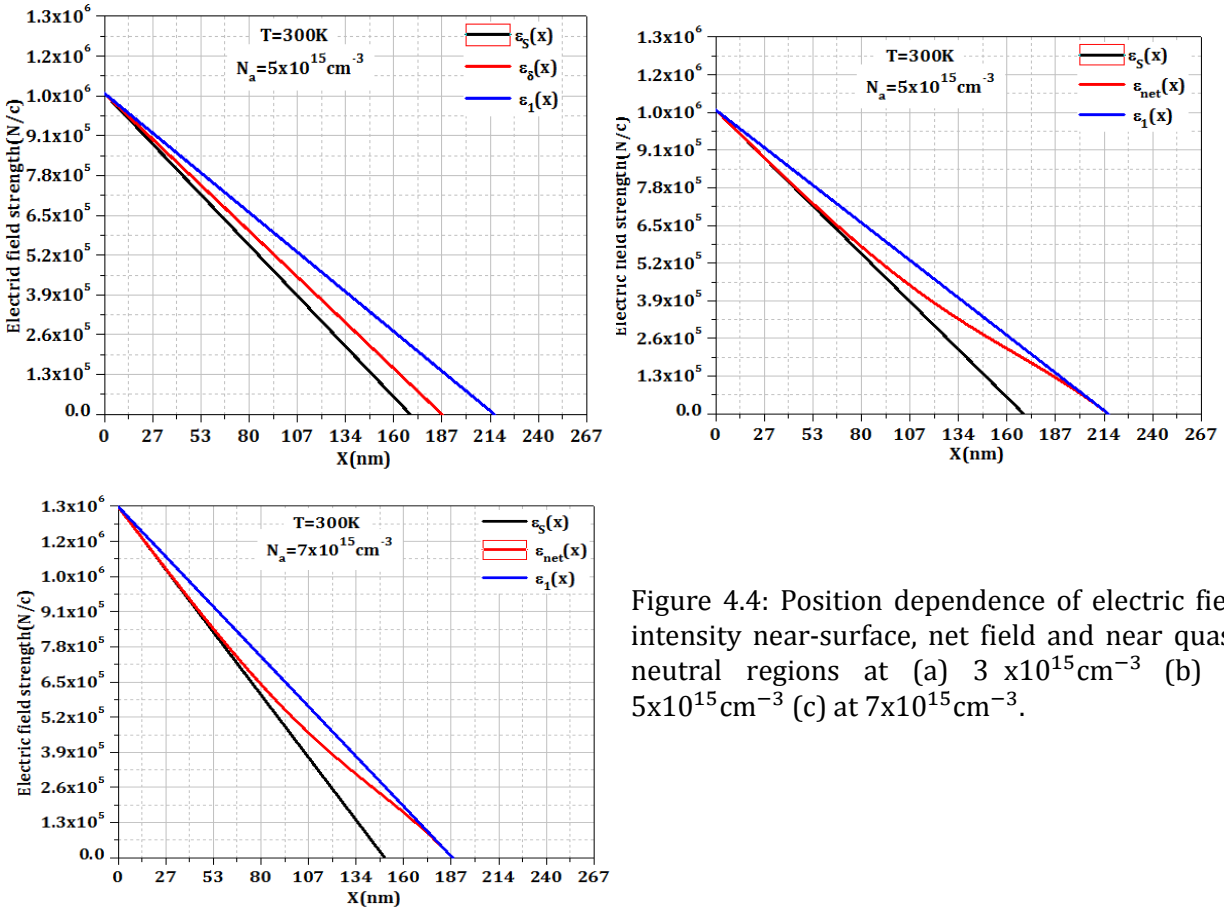

Figure 4.4: Position dependence of electric field intensity near-surface, net field and near quasi-neutral regions at (a) 3 x10^{15}cm^{-3} (b) at 5x10^{15}cm^{-3} (c) at 7x10^{15}cm^{-3}.

Figure 4.4 shows the position dependence of the electric field in the entire depletion region for various doping levels.

Figure 4.4 (a) portrays the three regions namely, the near-surface (black line), the transition layer (red line) and near the near quasi-neutral region (blue) provided by ε_1, ε_δ and ε_S respectively are performed using the relations in Eqn. (2-56). The doping level dependence of electric field versus position graph specified by the black line (ε_S) is the electric field strength near surface region which performs well only in the near-surface region.

The electric field line painted by the red line (ε_δ) is the electric field strength in the transition layer. that works well only in the transition layer. and it flops in the rest vicinities. The electric field graph indicated by the blue line (ε_1) is the net electric field strength near the quasi-neutral region. which performs well near the quasi-neutral region.

The three considerations on the choice of the positions in the entire depletion region the fields work well in their respective positions.

The present study implied the findings of the electric field in the depletion region is linearly dependent on the position. Our results demonstrated that the electric field assumption of the three cases confirm the field is linearly varying with the depth of the depletion region. For uniformly doped semiconductors, the electric field is linearly varying with the depth across the depletion region. This result is in line with the previous studies conducted. For a uniformly doped semiconductor, the electric field is linearly varying with distance across the depletion region [23].

However, the net electric field $\varepsilon(x)$, indicated in Figure 4.4 (b) and (c), by the red lines drawn using Eqn. (2-56) in the literature section. The ultimate result in this section is that the electric field intensity is not linearly varying with position, rather it is a deviated line from linearity just after the near-surface region to the quasi-neutral region.

4.5 The minority carrier lifetimes versus depth in the depletion region for different doping levels

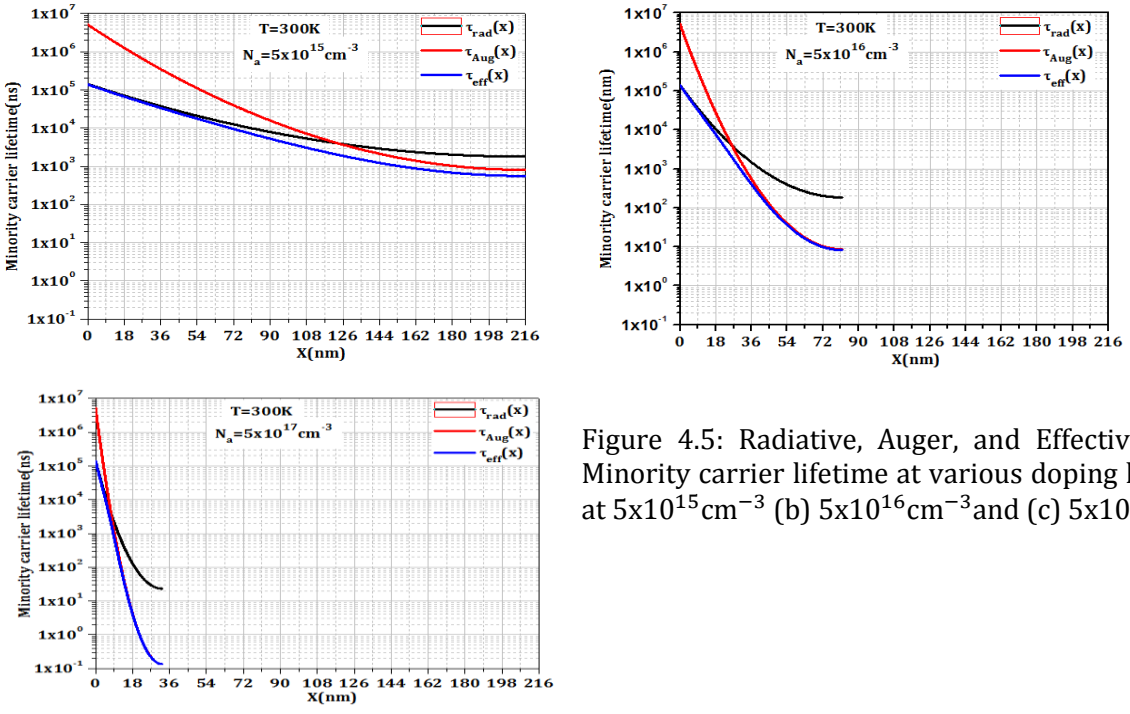

Figure 4.5: Radiative, Auger, and Effective Excess Minority carrier lifetime at various doping levels (a) at $5x10^{15}cm^{-3}$ (b) $5x10^{16}cm^{-3}$and (c) $5x10^{17}cm^{-3}$

The band-to-band recombination is the name for the process of electrons jumping down from the conduction band to the valence band in a radiative manner. Radiative recombination occurs when an electron in the conduction band recombines with a hole in the valence band and the excess energy is emitted in the form of a photon. Radiative recombination is thus the radiative transition of an electron in the conduction band to an empty state (hole) in the valence band.

Auger recombination is a non-radiative process involving three carriers. Direct Auger recombination occurs when an electron and hole recombine, but instead of producing light, either an electron is raised higher into the conduction band or a hole is pushed deeper into the valence band.

Minority carrier lifetime is the average time it takes for minority excess carriers to be eliminated. The three-minority excess carrier lifetime is the radiative, the Auger and the effective carrier lifetime.

Figure 4.5 indicates as the doping level increases, the magnitude of the minority carrier lifetime decreases. This means the higher the doping level the smaller is the meantime for electron-hole-pairs to disappear.

However, the radiative excess carrier lifetime near the surface is closer to the effective minority carrier lifetime. This depicts that the radiative excess carrier lifetime dominates the region near-surface to the highly depleted region. The region from the edge of the transition layer to the quasi-neutral region is, however, dominated by the Auger excess minority carrier lifetime. In general, the values of the effective excess carrier lifetimes, for the given samples with doping levels of $5x10^{15}cm^{-3}$, $5x10^{16}cm^{-3}$ and $5x10^{17}cm^{-3}$ varied from $1.34x10^{-1}ns$ to $1.38x10^{5}ns$.

Chapter 5 : Conclusion

This thesis is aimed at determining the effects of the doping levels on the electrical properties of the near-surface depletion region of Gallium antimonide semiconductor. The position-dependence density of free carriers, energy band bending, electric field strength, charge density, and minority carrier lifetime the near-surface depletion region were studied.

One of the ultimate results of this thesis is the net (average) electric field in the depletion region varies non-linearly with position. However, the results indicated the field varied linearly in the near-surface and bends until the edge of the quasi-neutral region. The slanted line indicates the net electric field in the depletion region does not vary linearly with position. Therefore, our results prove the net electric field produced in the depletion region of semiconductors do not vary linearly with position.

The majority carrier concentration as a function of position increases exponentially as the doping level increases. The concentration is minimum at the surface, slightly increases at the edge of the transition layer and gets its maximum value at the edge of the quasi-neutral region. On the contrary, the minority carrier concentration is minimum at the quasi-neutral region and maximum at the surface region while the intrinsic carrier concentration remains unchanged in cases.

Moreover, the average charge density of free carriers as a function of position remains linearly varying at low doping concentration while at high-level doping it increases exponentially. But the net charge density of free carriers as a function of position exponentially increasing with the doping level with a higher magnitude compared to the average charge density.

The energy band bending in the depletion region for p-type semiconductor is a parabola that opens down due to the attraction of free electrons towards the surface and the distribution of the holes moved towards the bulk due to the net electric field generated in the depletion region. The band bending takes its maximum value at the surface whereas, it becomes minimum at the quasi-neutral region. The band bending is maximum at the surface and

minimum at the edge of the quasi-neutral region. Our result also confirms band bending increases as the doping concentration increases.

The excess minority carrier lifetime decreases with increasing the doping levels. The radiative excess carrier lifetime dominates the near-surface region (highly depleted region) whereas, the auger excess carrier lifetime dominates the rest region. To this end, we can also conclude that the depletion width decreases as the doping level increases.

References

[1] B. R. Bennet, "Antimonide-Based Compound Semiconductors for Electronic Devices," *journal of Solid-State Electronics,* vol. 49, no. 12, pp. 1875-1895, 2005.

[2] J. Ward, "Transistor Museum," in *Historic Semiconductors Research and Collecting Kit*, 2014, pp. 1-29.

[3] F. F. Sizov, "Brief history of THz and IR technologies," *Optoelectronics and optoelectronic devices,* vol. 22, pp. 67-69, 2019.

[4] J. V. Gorkon, "Advances in Imagingand Electron Physics," in *The Early Electron Microscopes: Incubation*, vol. 208, Elsevier, 2018, pp. 43-128.

[5] M. Riordan, "The invension of transistor," *Journal of applied physics,* vol. 71, no. 2, pp. S336-S345, 1999.

[6] N. Robert, "Robery Noyce and Fairchild Semiconductor, 1957-1968," *Business History Review,* vol. 75, no. 1, pp. 63-101, 2001.

[7] D. A. Neamen, Basic principles of Semiconductor Physics, 4 th ed., New York: The McGraw-Hill Companies, Inc., 1221, 2012, pp. xvii-xix.

[8] M. Cardona, Fundamentals of semiconductor: physics and materials properties, 4th ed., London: Springer, 2010.

[9] B. G. Yacobi, Semiconductor materials: An introduction to basic principles, vol. 1, Toronto: Klumber academic publishers, 2003, pp. 1-3.

[10] B. G. Banerjee, Solid State Electronic devices, 6 th ed., vol. M97, New Delhi: Asoke K. Ghosh PHI Learning Private Limited, 2009.

[11] M. A. Rahman, "A review on semiconductor including applications and temperature effects in semiconductors," *Journal for Engineering, Technology, and Sciences,* 2014.

[12] G. L. Pearson, "proc. Proceedings of the IRE," vol. 43, no. 12, pp. 1794-1806, 1995.

[13] S. M. Sze, Physics of Semiconductor Devices, third ed., Wiley and sons, 2006.

[14] B. Mitchell, An Introduction to materials engineering and science, Hoboken: New Jersey, John Wiley and sons, 2004, pp. 550-557.

[15] J. R. Meyer, "Band parameters for III-V compound semiconductors and their alloys," *Journal of Applied physics,* vol. 89, February 2001.

[16] Y. B. Kim, "Challenges for NanoscaleMOSFETs and Emerging Nano Electronics, Transactions on Electrical and Electronic Materials," *Journal of computer and elecrical engineering,* vol. 11, no. 1, pp. 93-105, 2010.

[17] D. Y. Peide, Fundamentals of III-V semiconductor MOSFETs, New York: Springer, 2010, pp. 15-21.

[18] J. R. Chelikowsky, "Electronic Structure and Optical Properties of Semiconductors," *Jounal of solid state physics,* 1988.

[19] T. Kikkawa, "Spectroscopic Studies of III-V Semiconductor Materials for Improved devices," *Fujitsu Science and Technology Journal,* pp. 40-48, 2012.

[20] C. W. Wilmsen, "Physics and Chemistry of III-V Compound Semiconductors interfaces," *Applied Physics,* pp. 339-342.

[21] A. H. Kroemer, "The 6.1 Å family (InAs, GaSb, AlSb) and its Heterostructures:," *a Selective Review Physical Electronics,* vol. 20, pp. 196-203, 2004.

[22] Hideharu MATSUURA and et.al., "Acceptor Densities and Acceptor Levels in Undoped GaSb Determined by Free Carrier Concentration Spectroscopy," *Japan Journal of Applied Physics,* vol. 41, no. 2A, pp. 496-500, February 2002.

[23] K. Wakita, Semiconductor Optical Modulators, 85-87 ed., New York: Kluwer Academic publishers, 1998.

[24] P. J. Simmonds, "Brief Review of Epitaxy and Emission Properties of GaSb and Related Semiconductors," *Crystals,* vol. 337, no. 7, pp. 1-21, 2017.

[25] A. Shaheen, W. Zia and M. S. Anwar, "Band structure and electrical conductivity in semiconductors," pp. 1-25, 2010.

[26] R. K. Willardson, "Energy band structure of mixed crystals of III-V compounds," *Semiconductors and semimetals,* vol. 1, p. 500, 1966.

[27] B. MAHMAN, "Structural Characterization of Gallium Antimonide Semiconductor used in air space station," Sefako Makgatho Health Sciences University, 2015. [Online]. Available: http://www.hindawi.com/journals/anse/2010/923409.

[28] N. K. Udayashankar, "Growth and characterization of indium antimonide and gallium antimonide crystals," *Bulletin of material science,* vol. 24, p. 445, 2001.

[29] R. W., The solid state ElectronIc Materials, vol. 30, 2001, p. 1429.

[30] P. Hidalgo, "Material Science and Engineering," *Applied Physics,* vol. B81, p. 157, 2001.

[31] V. Nahirnyak, "Gallium antimonide (GaSb)," in *Christal structure*, 2002, pp. 1-7.

[32] C. Kettel, Introduction to solid state physics, eigth edition ed., New York: John Wiley and sons, 2005, pp. 216-226.

[33] J. Piprek, Semiconductor Optoelectronic Devices Introduction to Physics and Simulation, California: Academic press, 2013.

[34] P. Kuiper, "Comparison of the electronic band structures of metals, semiconductors and insulators," 2007. [Online]. Available:https://commons.wikimedia.org/wiki/File:.

[35] K. P. O'Donell, "Temperature dependence of semiconductor band gaps," *Applied physics,* vol. 58, p. 2924, 1991.

[36] Y. P. Varshni, "Temperature dependence of the energy gap in semiconductors physics," *Physica,* vol. 34, pp. 149-154, 1967.

[37] B. Pejova, "Temperature Dependence of the Band-Gap Energy and Sub-BandGap Absorption Tails in Strongly Quantized ZnSe Nanocrystals Deposited as Thin Films," *physical chemistry,* vol. 114, no. 36, pp. 15280-15289, 2010.

[38] M. L. Nakarmi, "Temperature and compositional dependence of the energy band gap of AlGaN alloys," *Applied physics,* vol. 87, p. 242104, 2005.

[39] P. Sarswat, "A study of energy bang gap versus temperature for Cu2ZnSnS4 thin films," *Jornal of condnsed matter,* vol. B407, pp. 108-111, 2012.

[40] N. Nepal, "Temperature and compositional dependence of the energy band gap of AlGaN alloys," *Applied physics,* vol. 87, p. 242104, 2005.

[41] M. W. Shura, "Energy bands of crystalline solids," in *Semiconductor Fundamentals unpublished material*, 2017, pp. 1-214.

[42] M. L. Free, "A Study of Energy Band Gap Temperature Relationships for Cu2ZnSnS4: Thin Films," *Journal of Thin Film Optical Properties.,* pp. 1-8.

[43] *The Effect of Hydrogen Passivation on Heteroepitaxial Gallium Antimonide Grown on Silicon and Versulite Substrates M.S Thesis, University of Vermont Electrical Engineering,* 2006.

[44] "Physico-Technical Institute of the Ioffe. Gallium Antimonide Band Structure and Carrier concentration".

[45] A. Y. Polyakov, "Hydrogen effect on shallow and deep centers in GaSb," *Journal of applied physics,* vol. 60, no. 11, 1992.

[46] L. L. Li, "Mid Infrared Absorption by Short-Period InAs/GaSb type II superlattices"," *Journal of Microelectronics,* vol. 40, no. 4-5, pp. 815 - 817, 2009.

[47] F. B. a. L. Dehimi, "Performance evaluation of a GaSb thermophotovoltaic converter," *Journal of Metallic and Semiconducting Materials,* vol. 15, no. 3, pp. 383-397, 30 September 2012.

[48] Y. Z. Hu, Theory of optically excited intrinsic semiconductor quantum dots, vol. B42, 1990.

[49] S. M. Sze, Physics of Semiconductor Devices [a comprehensive advanced text], New York: Wiley and sons, 1981.

[50] P. F., Advanced Semiconductor Fundamentals, in Modular series on solid state devices, vol. 6, 1987.

[51] A. A. Mermin, Solid State physics in sounders, Philodelphia, 1976, pp. 76-81.

[52] A. Shaheen, Band Structure and Electrical Conductivity in Semiconductors, 2010.

[53] G. Stollwerk, "GaAs/GaSb Tandem Concentrator solar cell," *proc.14TH European PVSEC,* no. 14, pp. 993-998, 1997.

[54] T. M. S., Introduction to Semiconductor Materials and Devices, New York: Wiley and sons, 1991.

[55] C. Kettel, Introduction to solid state physics, seventh edition ed., Wiley and sons, 2010.

[56] S. Wang, Fundamentals of Semiconductor Theory and Device Physics, vol. 1, Englewood: Prentice-Hal, 1989.

[57] A. Carvalho, "Donor and Acceptor Levels in Semiconducting Transition Metal Dichalcogenides," *Condensed Matter Mes-hall,* pp. 1-6, 2013.

[58] M. Grundmann, Physics of Semiconductors, An introduction including Nano Physics and Applications, Verlag: Springer, 2010.

[59] P. B. &. J. W. Orton, "The Electrical Characterization of Semiconductors: Major Carriers and Electron States".

[60] J. Ma., "Carrier density and compensation in semiconductors with multiple dopants and multiple transition energy levels: Case of Cu impurities in CdTe," *Journal of phsical review,* vol. B83, pp. 245207-245113, 2011.

[61] P. Ravindran, "Carriers Concentration in Semiconductors - IV," in *Semiconductor Physics*, vol. IV, 2014.

[62] J. M. Borrego, "Recombination Parameters for Antimonide-Based emiconductors using RF Photoreflection Techniques," *Journal of Electrical, Computer and Systems Engineering,* 10 October 2002.

[63] W. M. Saslow, "Electricity, magnetism and light," Elsevier, 2002.

[64] F. Rana, "Intersubband trasition based processes and devices in AlN/GaN-based heterostructures," 2010.

[65] B. J. Skromme, "Encyclopedia of Materials:," *Jounal of Science and Technology,* vol. 2, pp. 1-19, 2004.

[66] S. K. Ghandi, Semiconductor Power Devices, New York: Wiley and sons, 1977.

[67] J. J. Sparkes, "Semiconductor devices, second edition, London," 1994.

[68] I. A. Babalola, "Surface and interface states of GaSb: A photoemission study," *Physical review,* vol. B15, 15 February 1977.

[69] S. S. Li, "Excess carrier phenomenon in semiconductors," in *Semiconductor physical electronics*, pp. 134-170.

[70] S. G. A. Wincukiewiz, "Radiative recombination and other processes related to excess charge carriers, decisive for efficient performance of electronic devices," *Lithuanian Journal of Physics,* vol. 58, no. 1, pp. 49-61, 2018.

[71] A. Haug, "Auger recombination in quantum well gallium antimonide," *Journal of Physics C :Solid State Physics,* no. 20, pp. 1293-1299, 1987.

[72] W. K. M. a. M. W. Wanlass, "Auger recombination in low-band-gap n-type InGaAs," *Applied Physics letters,* vol. 79, no. 20, pp. 3272-3274, 24 January 2001.

[73] J. R. Poindexter, "Charge-carrier lifetime measurements in early-stage photovoltaic materials: intuition, uncertainties, and opportunities," pp. 1-20.

[74] P. C, "A comparison of dominant recombination mechanisms in n-type InAsSb materials".

[75] J. R. B. a. M. C. Wagener, "Non-linear injection level dependence of the excess carrier lifetime of p-type GaSb thin films: A two-layer model," *Journal of applied physics,* vol. 111, 2012.

[76] J. M. B. P. S. D. R. J. G. C. A. W. e. a. R. J. Kumar, "Auger and radiative recombination coefficients in 0.55-eV InGaAsSb," *American Institute of physics,* vol. 97, 2005.

[77] K. T. Serdo, M. W. Shura, and T. L. Fole, "Effect of the Near Surface Depletion Layer on Photo-Response of Direct Band Gap Semiconductor," *Advances in Physics Theories and Applications,* vol. 75, pp. 1-17, 2019.